Chapter IV

Rapid selective optical detection of sulfur containing agrochemicals and amino acid by functionalized cyclodextrin polymer derived gold nanoprobes

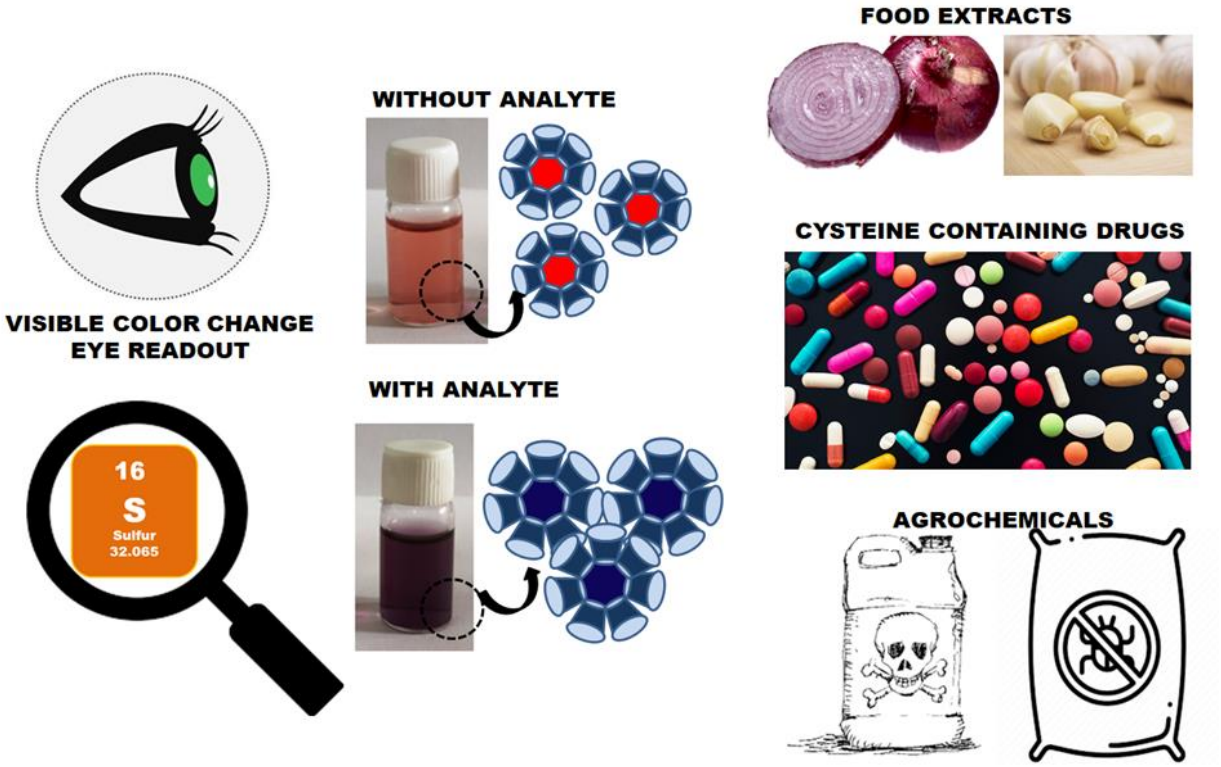

4.1. Introduction

Natural and anthropogenic process introduces various pesticides, chemical toxins, organic-inorganic pollutants, heavy metals etc. into the environment[1]. Persistence monitoring is required to secure a better water supply in public domain as well as to administer their effect on the ecosystem and environment[2]. Recognition and monitoring of various biological and chemical agents residing in the environment plays significant role in biomedical, forensic and environmental sciences applications [3–7]. Atomic absorption spectroscopy, electrochemical sensors, inductively coupled plasma atomic emission spectrometry etc. are some techniques that exhibit low detection limits but are expensive, time-consuming, sample destructive and complex. Therefore, on-site detection is not suitable with sophisticated instrument-based methods [8]. On the other hand, colourimetric and fluorometric methods based molecular probes and chemosensors are popular due to simple operational activity. The visual readout methods are employed depending on unique optical properties such as surface plasmon resonance (SPR) exhibited by noble metal nanomaterials[9–11]. Sensors commonly have two functional components i.e. a recognition element and transducer; the recognition element binds specifically with analytes and transducer signals the binding process. The sensor efficacy relies on the above-mentioned components for remarkable sensing on the basis of the limit of detection, response time, selectivity etc. Therefore, the efficient sensor synthesis depends on generation of new materials with better recognition and transduction processes. The nanomaterials imparts various unique physicochemical properties in case of chemical and biological sensors, helping in generation of novel transduction and recognition processes [4]. The nanomaterials have been utilized as an active component for sensing that exhibits better results depending upon their unique properties. Various optical sensors based on nanomaterials have been reported by researchers such as carbon dots, upconversion nanoparticles, quantum dots, metal oxide nanomaterials, gold and silver nanoparticles, organic fluorescent molecules based-nanomaterials and nanozymes [12,13]. A well-defined chemical and physical characteristic has been sustained by gold nanoparticles constructing a better scaffold to synthesize novel chemical as well as biological sensors [14,15]. The physicochemical properties of Gold nanoparticles as transducer could be modified during binding with sensor and analyte [16]. The gold nanoparticles possess LSPR band that could be utilized for colourimetric assessment of metal ions, amino acids, DNA, pharmaceutical compounds, proteins etc. as well as the formation of microscale optical devices [17–21].

Cysteine is an important sulfur-containing amino acid that manages several cellular activities mainly in metabolism, detoxification, protein folding etc. [22]. Therefore, recently the detection of cysteine has gathered the special interest of researchers. Since sophisticated instruments based methods are complex and less sensitive, therefore, rapid and specific determination of cysteine using chemosensor is of great interest [23]. Some instrument-based methods have been reported for the purpose of cysteine detection [24–26]. Whereas some chemosensors have been synthesized depending upon the aggregation of gold nanoparticles [27–29]. However, very few gold nanoparticles based chemosensors have been developed for sensitive, rapid as well as selective detection of cysteine.

Similarly, dithiocarbamate, is commonly used organosulfur compound in wood preservative, agricultural pesticides, as vulcanization additive in the rubber industry etc. The detection of sulfur-containing analytes in water as well as other environmental samples is an imperative tool to detect pesticides. For instance, several gold nanoparticle-based colourimetric sensors have been previously reported for the detection of pesticides like chlorpyrifos, organophosphates, dimethoate, pymetrozine, etc [30–33].

In this work, the facile, robust and rapid colourimetric method has been developed utilizing a stable gold nanoparticle-based sensor synthesized by cyclodextrin crosslinked polymer with phthalic anhydride (CDPA). Herein, we have implemented the unique ability of beta-cyclodextrin (β-CD) that binds with both hydrophilic and hydrophobic compounds [34,35]along with Au-thiol interactions. The sensing of amino acid (i.e. Cysteine) as well as agrochemical (i.e. diethyldithiocarbamate) has been accomplished by using nanosensor. The colourimetric assessment of nanosensor shows red shift (from 524nm to 670nm) within 5 seconds for sulfur-based compounds. A detailed qualitative and quantitative study of Cysteine and Sodium diethyldithiocarbamate sensing was carried out. Various analytical characterizations proved the mechanism of sensing unveiling the role of functionalized cyclodextrin. The simple, rapid and selective detection of the sulfur compound was demonstrated utilizing pesticide samples as well as allicin, a reported agrochemical present in extracts of onion and garlic. Silver based nanosensor was also synthesized for comparison study. The efficacy of gold nanosensor was found to be much superior in comparison to silver-based nanosensor.

4.2. Materials and Methods

4.2.1. Materials

Gold (III) chloride hydrate ($HAuCl_4$) and silver nitrate ($AgNO_3$) was purchased from Spectrochem, India pvt. Ltd. β- Cyclodextrin (≥ 97% purity), Sodium hydride (NaH), Cysteine (Cys), Proline (Pro), Glycine (Gly) and Phthalic anhydride (PA) were purchased from Sigma Aldrich, India. N, N Dimethylformamide (DMF) was purchased from Qualigens, Bombay, India. NaCl was purchased from Molychem, Mumbai, India. Sodium diethyldithiocarbamate (SDDC), Thioglycolic acid (TGA), Sodium metabisulfite (SMB) and Ammonium thiocyanate (ATC) were purchased from Loba Chemie, Mumbai, India. Solid and liquid pesticide samples were collected from a local plant nursery. Analytical grade reagents were used as received.

4.2.2. Characterization

Gold nanoparticles were characterized using UV–vis spectroscopy measurements performed on Cary 60 UV-Vis spectrophotometer (Agilent Technologies). The morphology measurements of the nanosensors were carried out on a High-Resolution Transmission Electron Microscopy (HR-TEM) analysis Jeol (Jem-2100) electron microscope at an acceleration voltage of 200 kV.NMR spectrum for CDPA polymer was recorded on Bruker Avance III (400 MHz) NMR spectrophotometer using D_2O as the solvent. PerkinElmer IR spectrophotometer was used to record FTIR spectra of nanosensors before and after the addition of analytes. The size distribution was analyzed by dynamic light scattering measurements (DLS) recorded on Beckman Coulter Delso Nano. The zeta potentials of nanosensors before and after analytes addition were measured with Malvern Zetasizer (Nano-ZS 90). FESEM-EDX was recorded on JSM7600F.

4.2.3. Synthesis of Au and Ag derived nano-sensors

4.2.3.1.CDPA polymer synthesis

The crosslinked cyclodextrin phthalic anhydride (CDPA) polymer has been synthesized as per the previously reported procedure[36]. Briefly, 1.13 g, 0.001 mol of CD was dissolved in 20 ml of DMF and this solution was maintained at 0-5 °C in an ice bath. To the chilled CD solution 0.16 g, 0.007 mol of sodium hydride (NaH) was added slowly under vigorous stirring. The stirring was continued under cold conditions for 30 minutes. The temperature of the reaction was raised to 37 °C and continued at this temperature for 6 h to assist the formation of CD oxoanion

species. After the completion of 6 h, a gel-like polymer was observed; this confirmed the formation of oxoanion. To this solution 1.62 g, 0.011 mol of phthalic anhydride was added and the temperature of the reaction mass was increased to 130 °C. The reaction was allowed to proceed at 130°C for 1 h. Upon completion of 1 h, the reaction mass was cooled and CDPA polymer was precipitated from the reaction mass using acetone. The polymer was purified by a re-precipitation method using acetone thrice. The final CDPA (0.95 g) polymer was obtained as brown solid, dried and stored under vacuum until further use.

4.2.3.2.Synthesis of Au derived functional nano-sensor AuNS@CDPA

For the synthesis of AuNS@CDPA, CDPA polymer was introduced as a novel ligand for the fabrication of aqueous dispersed gold nanoparticles. The 0.001 M of the gold solution was prepared by dissolving the calculated amount of $HAuCl_4.3H_2O$ in deionized water. Typically, 10 mg CDPA polymer was dissolved in conductivity water followed by the addition of 1.0 mM gold solution dropwise on continuous stirring for 1 h. The formation of gold nanoparticles is marked by change in colour of solution from yellow to wine red.

4.2.3.3.Synthesis of Ag derived functional nano-sensor AgNS@CDPA

For the synthesis of AgNS@CDPA, the calculated amount of $AgNO_3$ was dissolved in deionized water to prepare a 0.01 M silver solution. 10 mg CDPA polymer was dissolved in conductivity water proceeded by adding 10.0 mM silver nitrate solution dropwise on continuous stirring for 4 h. The synthesis was confirmed by the change in colour of solution from light-yellow to orange.

4.2.4. Preparation of Samples

0.1M stock solution of the analytes, cysteine (Cys), proline (Pro), glycine (Gly), sodium diethyldithiocarbamate (SDDC), thioglycolic acid (TGA), sodium metabisulfite (SMB), ammonium thiocyanate (ATC) was prepared in double-distilled water. Further, the serial dilutions were done to prepare a working solution in the range of 0.01 µM to 0.25 µM. To evaluate the efficiency of the sensor, a real sample of sulfur-based pesticides has been taken. 10mg solid pesticide (Phorente) was ground properly and dissolved in 5mL of distilled water, after centrifugation at 3000 rpm for 10 minutes, the extract was collected for the sensing experiment. In the case of liquid pesticide (Tafgor), 1 mL pesticide was diluted by distilled water up to 5 mL and analyzed for sensing.

4.2.5. The colourimetric sensing ability of AuNS@CDPA and AgNS@CDPA towards sulfur-based compounds

Analytical applications of nanosensors were measured by investigating absorption spectral changes in presence of sulfur-based analytes. In a typical experiment, each working solution (300 μL) has been introduced into 700 μL of nanosensor solutions (AuNS@CDPA and AgNS@CDPA). The visible colour changes were observed and subsequently, UV-visible absorption spectra of the solutions were recorded immediately. The absorption ratio A_{670}/A_{524} was used to estimate the concentration of Cysteine and SDDC for Au sensors. The selectivity of AuNS@CDPA towards sulfur-based compounds was evaluated in the presence of other non-sulfur compounds.

4.3. Results and Discussion

The realization of the unique physicochemical properties of gold nanoparticles (AuNPs) had led to the advent of its preparation via various physical and chemical techniques. The chemical method of synthesis mainly consisted of three major processes (i) preparation by citrate reduction (ii) stabilization with the sulfhydryl ligand and (iii) seed crystal growth method. However, the NPs prepared by these methods lack the presence of surface functionalities thus making them unsuitable for sensing applications[19]. Thus it becomes imperative to introduce a molecular functionalization to make the nanoparticles suitable for sensing specific molecules of choice. In addition to this, a covalent modification is best suited while preparing such functionalized nanoparticles to further improve the NP stability and to prevent removal of functionalizing agent under harsh conditions like high salt concentration, extremely acidic or basic media and at high temperatures[4].

With this purview, this work reports the synthesis of functional cross-linked polymer-stabilized gold nanoparticles as a colourimetric sensor for naked-eye detection. For enhancing the specificity of the sensor, the principle of host-guest chemistry was employed by introducing β-cyclodextrin (CD) as a primary component of the crosslinked polymer. CD is a well-known molecule capable of forming inclusion complexes with aromatic derivatives in its hydrophobic cavity and thus can be employed for developing selective detection sensors of aromatic derivatives. This ensures that the target analytes can be sensed based on structural differences in addition to their affinity for gold nanoparticles.

CD was crosslinked with phthalic anhydride by a facile one-step chemical reaction as shown in the scheme (**Figure 4.1**). The crosslinked CDPA polymer was then used as a capping agent for the functionalization of gold nanoparticles. It is noteworthy that there is no need to add a reducing agent to transform the entrapped gold ions into their nanoparticle form. Thus CDPA polymer is both a capping as well as a reducing agent. For comparison, a similar sensor system was prepared using Ag metal and CDPA polymer.

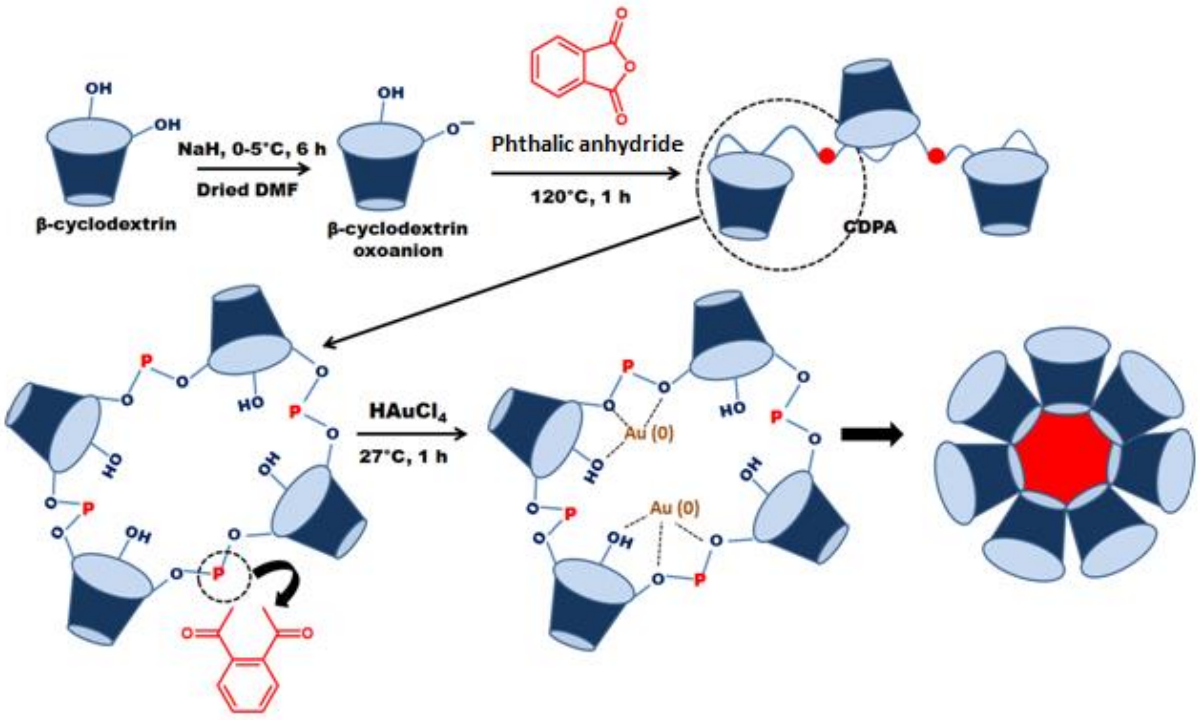

Figure 4.1: Schematic for synthesis of cyclodextrin phthalate ester (CDPA) polymer and subsequent entrapment of Au/Ag nanoparticles to form the nanosensor

4.3.1. Characterization of nano-sensors

The synthesized polymer CDPA, as well as CDPA functionalized Au and Ag sensors, were characterized by various analytical techniques as stated below:

4.3.1.1.NMR Analysis

The crosslinked CDPA polymer was characterized with ^{1}H proton NMR spectroscopy as shown in **Figure 4.2 (A)** [36]. The protons from repetitive units of β-CD's glucose units are observed at δ values in the range of 2.75 – 3.73 ppm [34]. The characteristic peaks for an aromatic phthalic ring

from the phthalic anhydride units appear in the range of 7.5 – 8.0 ppm [37]. This confirms the successful polymerization of CD with PA.

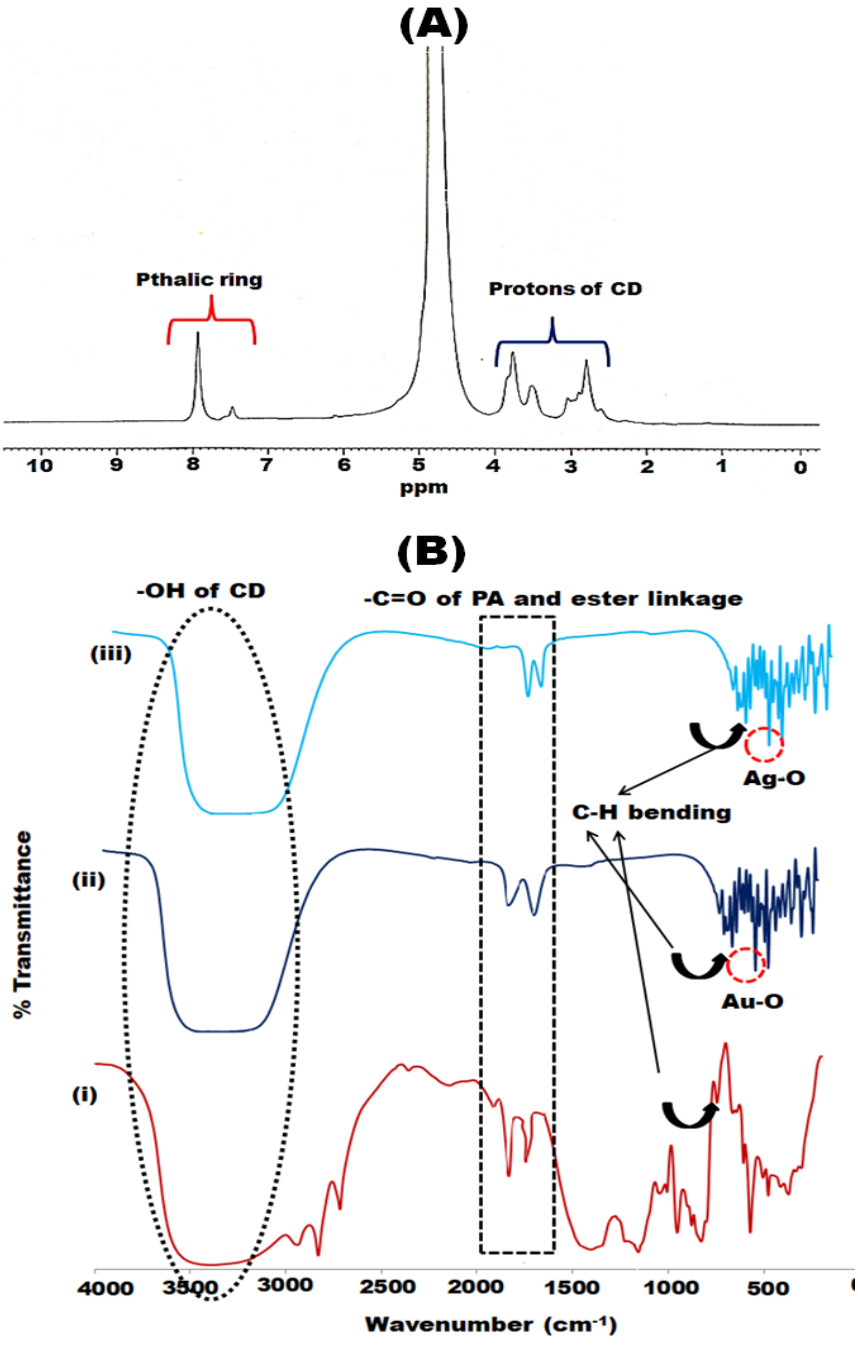

Figure 4.2: (A) ^{1}H NMR spectrum of CDPA polymer (B) overlay of FTIR spectra (i) CDPA polymer, (ii) AuNS@CDPA and (iii) AgNS@CDPA

4.3.1.2.FTIR Analysis

Figure 4.2 (B) represents the comparative IR spectra of CDPA polymer, AuNS@CDPA and AgNS@CDPA. The presence of a broad peak range of 3500-3300 cm^{-1} is the representative of the –OH group from β- cyclodextrin. The appearance of an absorption band at 1854 cm^{-1} corresponding to the carbonyl group of phthalic anhydride confirms the successful conjugation of CD with PA [38,39]. The successful pthalylation of CD is again confirmed by the appearance of a peak at 743 cm^{-1} that is a characteristic of the CH bending vibration of the o-substituted benzene ring [40]. The presence of a peak at 1760 cm^{-1} corresponds to the presence of carbonyl groups of ester linkages thus confirming successful esterification. The intensity of this ester carbonyl peak diminishes and shifts 1774 cm-1 and 1753 cm-1 in the case of AuNS@CDPA and AgNS@CDPA respectively. This indicates the involvement of carbonyl functionalities from ester linkage of the polymer matrix in the entrapment of Au/Ag ions and their subsequent stabilization upon reduction to NP form. The successful entrapment of Au and Ag is further confirmed by the appearance of peaks at 613 cm^{-1} and 627 cm^{-1} that can be assigned to Au-O and Ag-O vibrations [41].

4.3.1.3.UV-vis spectrophotometric determination

The AuNS@CDPA was prepared by various optimizations. The effect of polymer quantity on the spectral properties and stability was taken into consideration while synthesizing NPs with characteristics best suitable for sensing application [42].

The polymer was taken in various quantities as shown in **Table 4.1** and the quantity of $HAuCl_4$ solution was fixed at 1.0 mM.

Table 4.1: Optimization for preparation of AuNS@CDPA

Quantity of Polymer (mg)	Time taken for NP formation (min)	Nature of SPR peak[b]
1	300	Broad
3	280	Broad
5	180	Broad
7	60	Narrow
10	60	Narrow
15	60	Narrow

[a]150µL, 1.0 mM of $HAuCl_4$ was used; [b]SPR spectra were observed at 524 nm

Table 4.2: Optimization for preparation of AgNS@CDPA

Quantity of Polymer (mg)	Time taken for NP formation (s)	Spectral Property of the NPs[b]
1	330	Broad
3	240	Broad
5	200	Broad
7	150	Broad
10	100	Broad
15	60	Narrow
20	60	Narrow

[a]500µL, 10.0 mM of $AgNO_3$ was used; [b]SPR spectra were observed at 451 nm

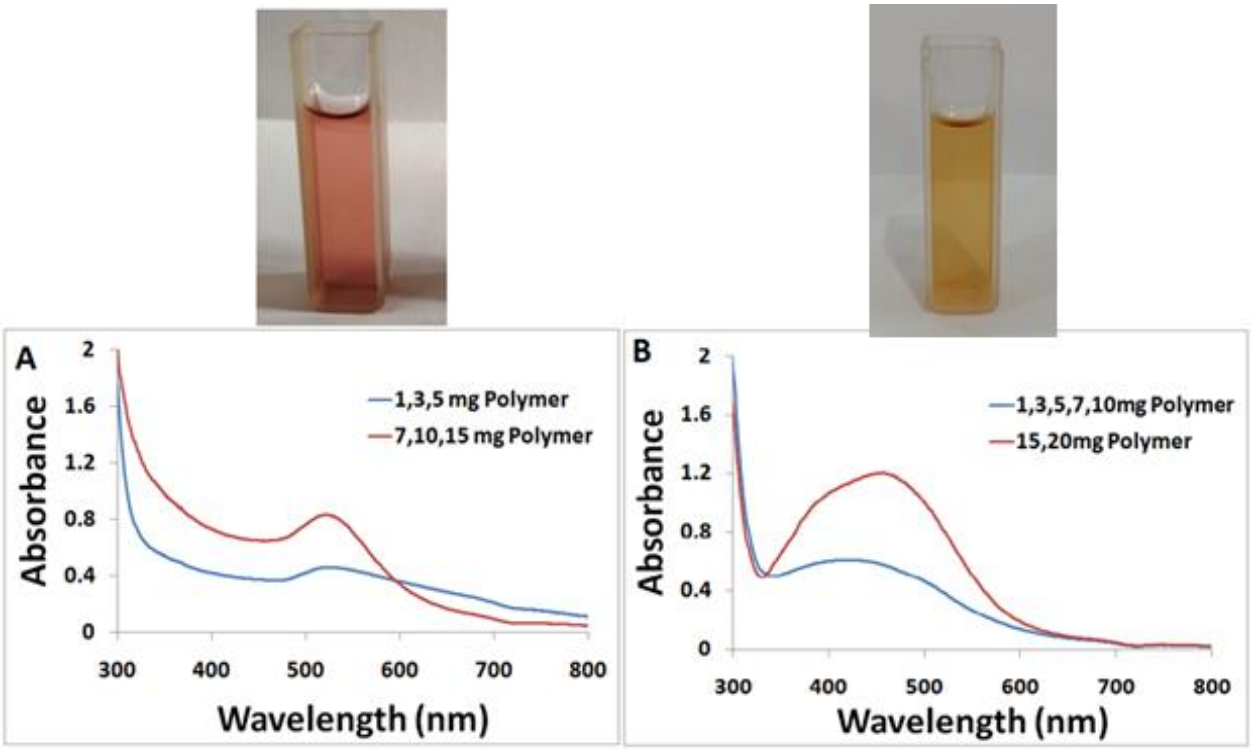

Figure 4.3: UV-vis determinations demonstrating spectral properties of synthesized nanoparticles (A) AuNS@CDPA and (B) AgNS@CDPA (inset images of cuvettes containing sensor solutions)

Similarly, when attempts were made for NP synthesis using $AgNO_3$ with these quantities, it was observed that 1mM solution did not yield desired nanoparticles. However, on increasing the concentration of $AgNO_3$ to 10 mM, the AgNS@CDPA nanoparticles were successfully obtained as shown in **Table 4.2**.

Based on these optimizations and with the analysis of SPR peak intensities, it was confirmed that 10 and 15 mg of the polymer was selected for preparing AuNS@CDPA and AgNS@CDPA respectively. The synthesized nanosensors under these conditions demonstrated maximum SPR intensity without any spectral broadening and representing the formation of uniformly sized nanoparticles as represented in **Figure 4.3**.

4.3.1.4.HR-TEM Analysis

The analysis of the size and morphology of AuNS@CDPA and AgNS@CDPA was performed by HRTEM imaging. The micrographs as shown in **Figure 4.4 (A&B)**, confirmed the presence of monodispersed nearly spherical nanoparticles. The mean diameter of both AuNS@CDPA and AgNS@CDPA was found to be in the range of 5-10 nm, with AuNS@CDPA having a size of 6 nm and AgNS@CDPA showed 11 nm. This also suggests that the particles remain uniformly dispersed in water and are devoid of agglomeration. This is also evident from the visual appearance of the sensor solutions which appear transparent as shown in **Figure 4.3**. Further, the lattice spacing observed on the surface of AuNS@CDPA and AgNS@CDPA was 0.27± 0.010 nm and 0.28± 0.013 nm respectively (as shown as inset images in **Figure 4.4 (A&B)**. These values corroborate with the standard{111}crystal plane of face centered cubic observed at 0.23 nm for Au/Ag nanoparticles[28].

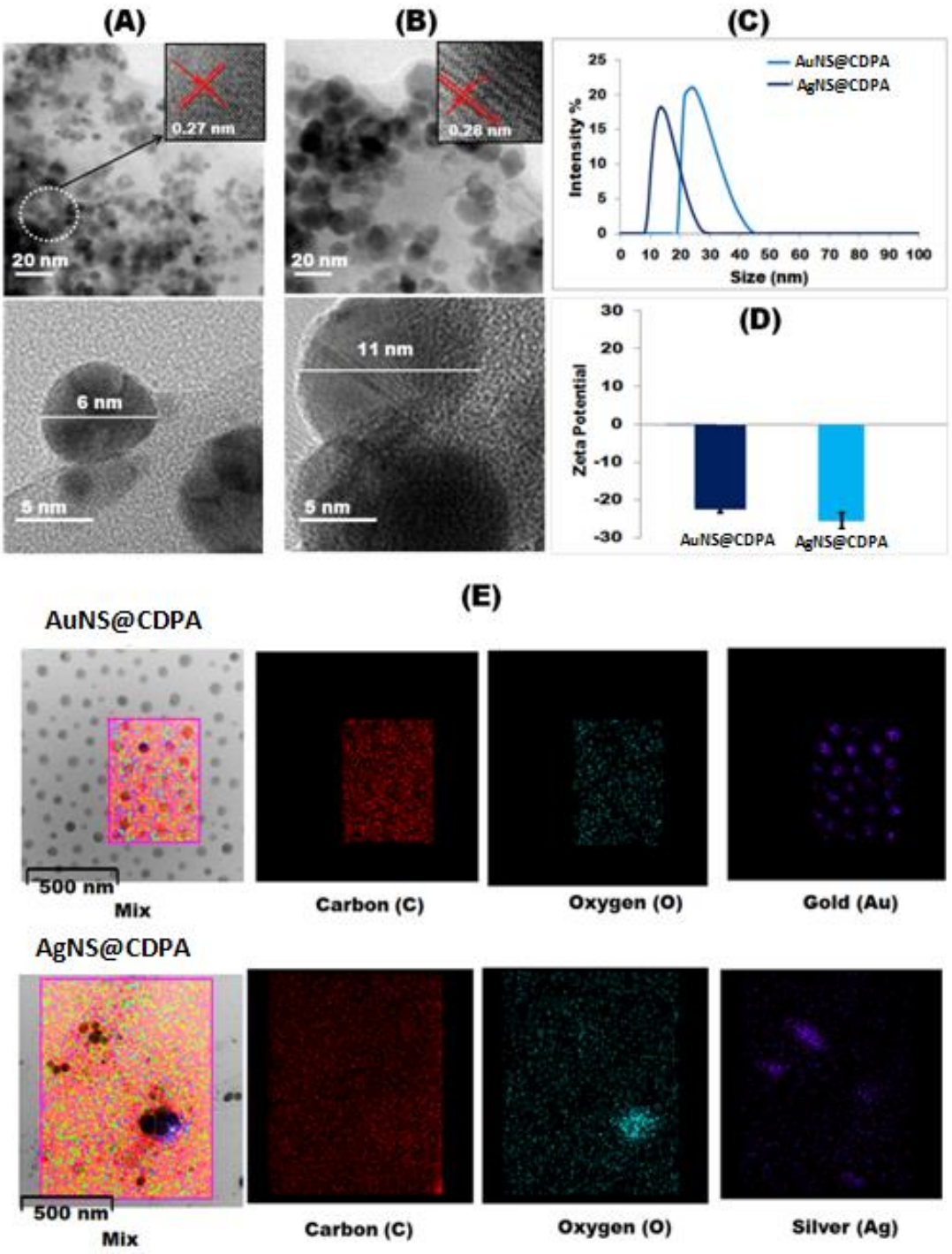

Figure 4.4: Characterization via HRTEM imaging for (A)AuNS@CDPA (B) AgNS@CDPA; comparison of the hydrodynamic size of both sensors via (C) DLS measurements (D) zeta-potential graph and (E) elemental mapping of the sensors

4.3.1.5. DLS and Zeta potential

For further size confirmation and to support the HRTEM analysis, the particle size of the sensors was also determined using DLS measurements. The results revealed an average hydrodynamic size of 13.2 nm for AuNS@CDPA and 24.3 nm for AgNS@CDPA **(Figure 4.4 (C))**. The smaller size of the particles observed in HRTEM measurements is attributed to the drying of the polymeric matrix during sample preparation. The zeta potential measurements demonstrated -21.23 mV and -25.62 mV for AuNS@CDPA and AgNS@CDPA respectively as shown in **Figure 4.4 (D)**. The surface negative charge is an attribute of free hydroxyl groups on the sensor surface and values close to -30 mV indicates good stability of the synthesized nanoparticles.

4.3.1.6. FESEM-EDX Analysis

The spherical morphology was further confirmed by FE-SEM imaging. The elemental mapping of AuNS@CDPA indicated a presence of 12% of elemental Au whereas AgNS@CDPA showed 10 % of elemental Ag. This ascertains the presence of Au and Au nanoparticles in the respective systems **(Figure 4.4 (E))**.

4.3.2. Colourimetric Detection of sulfur-based compounds

The presence of Au NPs in the sensor composition presents a potential of their capability in detecting sulfur-containing compounds. This is owing to the affinity of gold nanoparticles towards sulfur [42].

4.3.2.1. Sensing of Amino Acids

For the sensing experiments, the sensor solution was added to solutions of five different amino acids namely; glycine, proline, aspartic acid, tyrosine and cysteine. The solutions were analyzed for visual colour change along with spectral studies. The inset image of **Figure 4.3** representing AuNS@CDPA showed a wine red colour and demonstrated λ_{max} at 524nm. Upon addition of glycine, proline, aspartic acid and tyrosine no visible colour change was observed and the peak at 524 nm also remained persistent in these solutions. On the contrary, upon addition of cysteine into sensor solution, a distinct colour change from wine red to blue was observed within 5 seconds of addition. The UV-vis spectra also demonstrated a distinct change as shown in **Figure 4.5**.

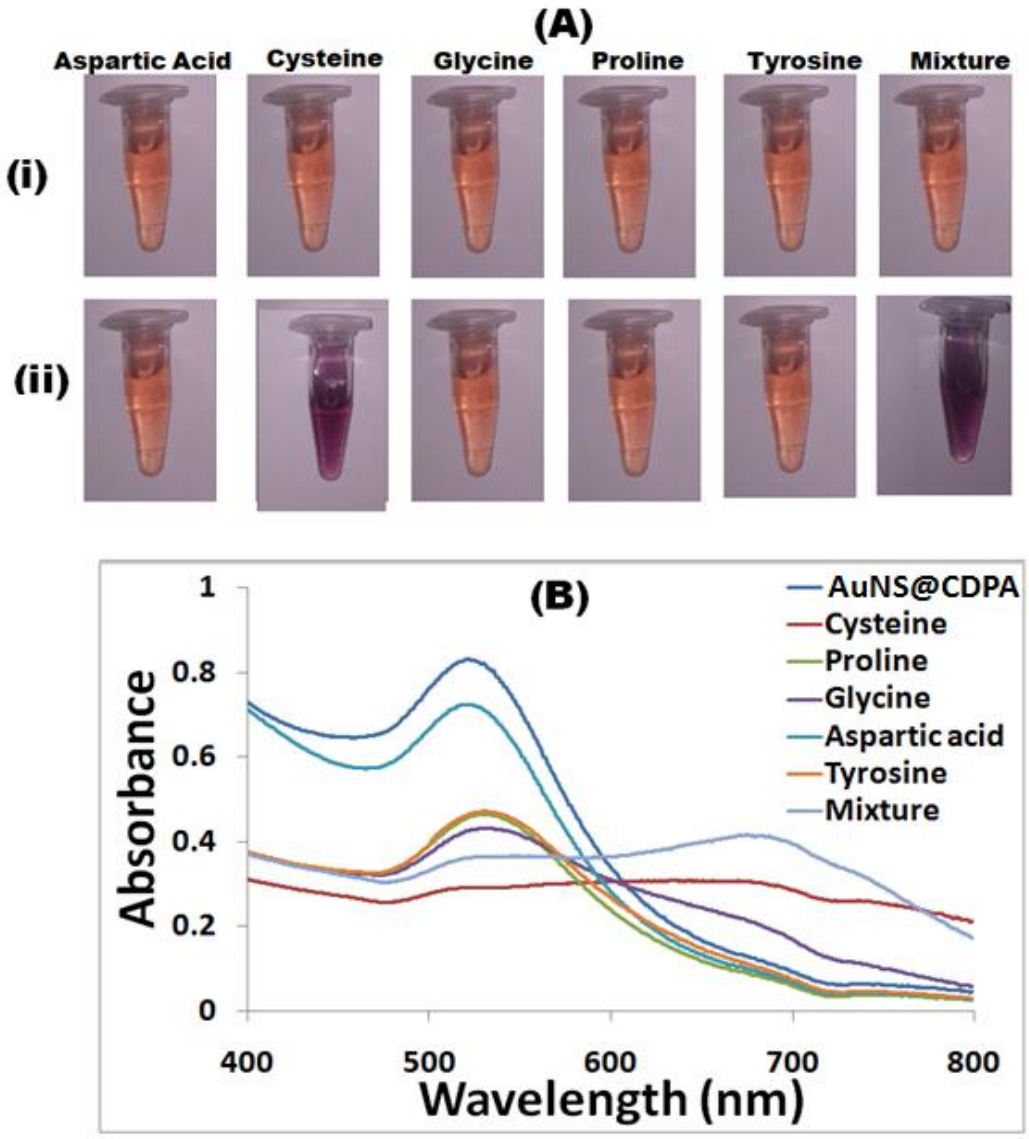

Figure 4.5: (A) Photographs and (B) Absorption spectra of AuNS@CDPA in absence and presence of various amino acids and their mixture

There was a drastic decrement in the intensity of SPR peak at 524 nm and in addition, there was an appearance of a new red-shifted peak at 670 nm. After the successful determination that the addition of cysteine can cause an alteration in the spectral signature of the sensor, its sensitivity towards the detection of cysteine was quantified. On increasing the concentration of cysteine to the sensor there is a decrease in the intensity of the peak at 524 nm and it completely disappears upon addition of 300 µL of 0.25 µM cysteine. However, a simultaneous increase in the peak intensity at 670 nm was observed with the increasing cysteine concentration. The cysteine

detection was quantified to 0.01 µM by calculating the absorption ratio of A_{670}/A_{524} nm and taking an average of three readings and preparing its plot against concentration. The change of colour and shifting towards a longer wavelength suggested an aggregation-induced increase in size and thus a shifting of SPR band upon cysteine addition.

Similar studies were carried out using AgNS@CDPA but no expected colour change or aggregation was observed (as shown in **Figure 4.6**).

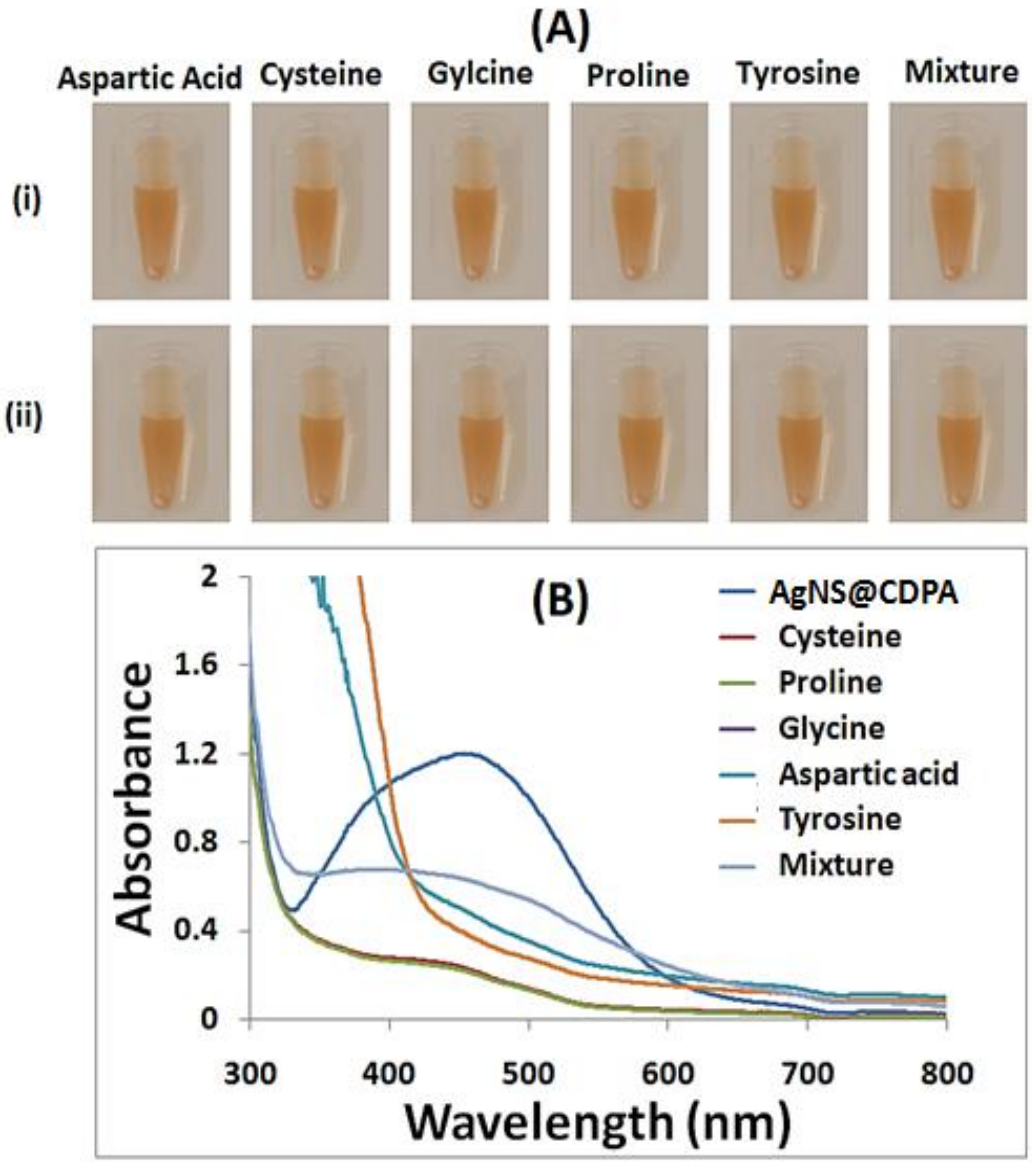

Figure 4.6: (A) Photographs and (B) Absorption spectra of AgNS@CDPA in absence and presence of amino acids (Cysteine, Proline, Glycine, Aspartic Acid, Tyrosine and Mixture)

4.3.2.2.Selective sensing of Cysteine in a mixture of amino acids

To investigate the selectivity of AuNS@CDPA towards sulfur-based amino acid i.e. cysteine, competitive sensing experiments were carried out with other non-sulfur based amino acids. A mixture of cysteine, aspartic acid, tyrosine, proline and glycine has been sensed using AuNS@CDPA. The absorption spectra ratio (A_{670}/A_{524}) was recorded and observed that only 300 µL of cysteine addition induced aggregation of gold nanoparticles. The UV-vis spectrum also represented a significant increase in absorption ratio. The selectivity of cysteine detection is due to the presence of the –SH group in its structure which has an affinity for gold. Any other amino acid does not possess SH groups and hence remain insensitive to the presence of the sensor. In the case of AgNS@CDPA, no colour change was observed in sulfur and non-sulfur based amino acids (cysteine, aspartic acid, tyrosine, proline and glycine). The visual inspection was also assisted by the UV-visible spectrum.

The results of these experiments suggest the selectivity of gold derived nano-sensor towards detecting sulfur-containing compounds. Thus the scope of this sensor was further extended to the detection of sulfur-containing agrochemicals that can act as potentially hazardous materials for the environment.

4.3.2.3. Sensing of Agrochemicals

Stock solutions of 10 mM were prepared of the following model analytes namely; potassium dihydrogen orthophosphate (PDO), sodium dihydrogen orthophosphate (SDO), di-sodium tetraborate (DST), sodium metabisulfite (SMB), di-ammonium hydrogen orthophosphate (DAHO), sodium hypochloride (SHC), diphenylamine (DPA), ammonium thiocyanate (ATC), thioglycolic acid (TGA), sodium diethyldithiocarbamate (SDDC). The solutions of sensing in micro-molar concentrations were then prepared by serial dilutions. The assessment of the sensing potential of agrochemicals using AuNS@CDPA and AgNS@CDPA was performed on these common chemicals used as pesticides or insecticides. Sensor solution (700 µL) was added to 300 µL of each of these analytes.

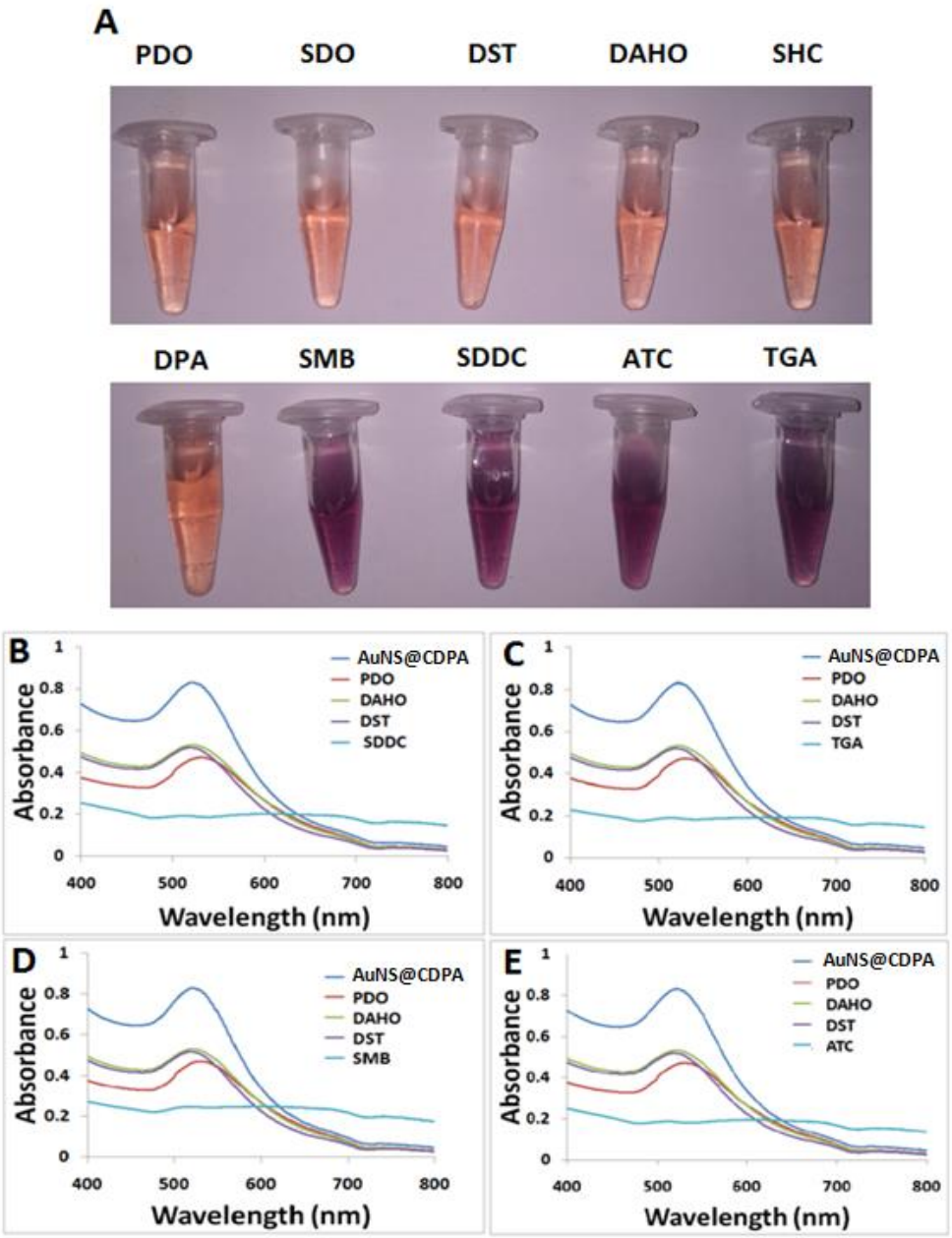

Figure 4.7: (A) Photographs of AuNS@CDPA solution in presence of different agrochemical compounds. The colour change is observed only in the case of sulfur-containing compounds (B-D) Comparative UV-visible spectra of AuNS@CDPA in a mixture of sulfur and non-sulfur agrochemicals

A colour change from wine red to blue was only observed in presence of sulfur-based agrochemicals i.e. SMB, ATC, TGA and SDDC whereas no such changes were observed with

non-sulfurous agrochemicals (**Figure 4.7 (A)**). The affinity of gold nanoparticles towards the sulfur group initiated the agglomeration resulting in colour change. Among sulfur-based compounds, SDDC represents the significant colour change in the lower concentration range; therefore, quantitative analysis of SDDC has been investigated. In the case of AgNS@CDPA, the addition of 300 µL of agrochemical solution into a 700 µL sensor represented no colour change, but there was a decrease in the intensity of the orange colour in the sensor solution probably due to its dilution.

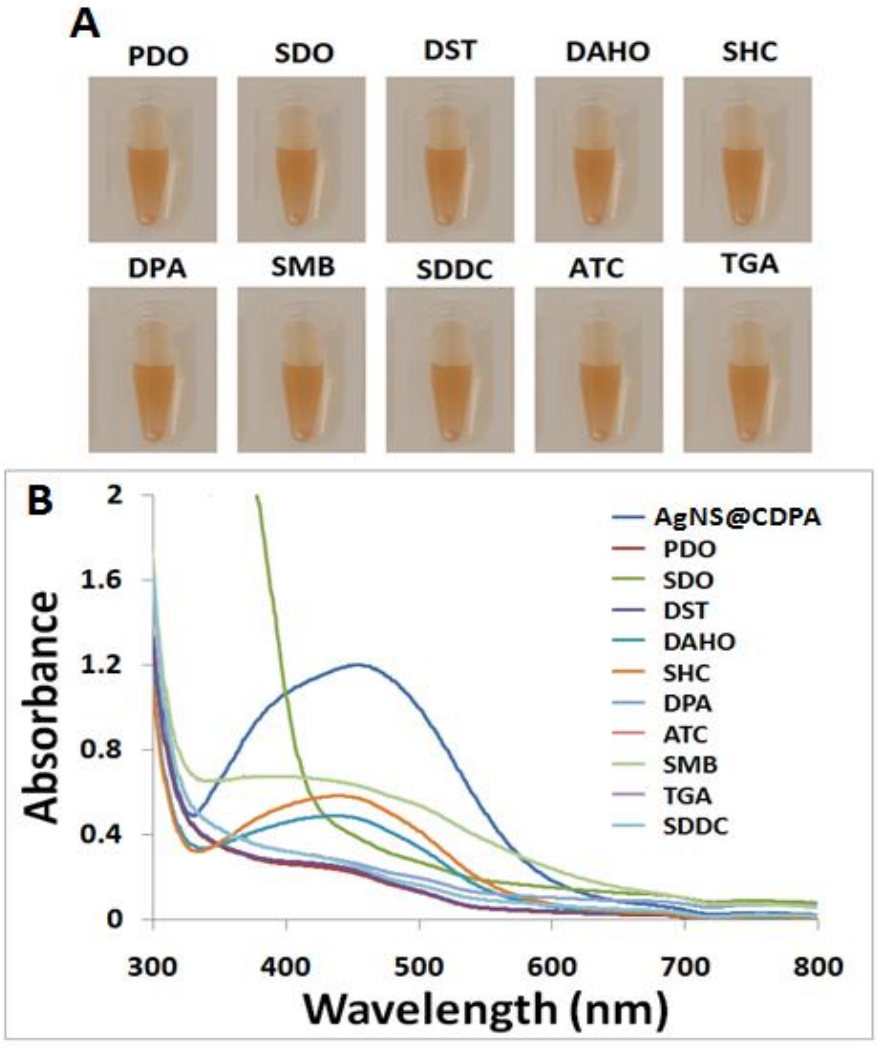

Figure 4.8: (A) Photographs and (B) Absorption spectra of AgNS@CDPA in absence and presence of agrochemicals (PDO, SDO, DST, DAHO, SHC, DPA, ATC, SMB, TGA and SDDC)

A rapid colour change in the SDDC solution is probably due to the reaction of a stable sodium diethyldithiocarbamate complex with AuNS@CDPA. A decrease in SPR absorbance was observed accompanied by a bathochromic shift arising from the influence that sulfur atom has on gold nanoparticles. Similarly, the dithiocarbamate compound containing the disulfide group also shows sensitivity towards the gold nanosensor. The quantification of SDDC detection was done based on an absorption ratio of A_{670}/A_{524} nm. The studies were performed in triplicate and average values were plotted against concentration. Since the rest of the chemical compounds did not have the presence of sulfur element in their structures they could not be detected using AuNS@CDPA.

The addition of agrochemicals in AgNS@CDPA solution imparts no significant visible colour change and observation was supported by UV-visible spectrum (**Figure 4.8**). These observations results suggested that AuNS@CDPA is a selective and suitable sensor for detection of such S containing analytes as compared to AgNS@CDPA.

4.3.2.4. Selective sensing of sulfur-based Agrochemicals in a mixture

To examine the selectivity of AuNS@CDPA towards sulfur-based agrochemicals, competitive sensing experiments were performed with non-sulfur based agrochemicals. In this investigation, PDO, DAHO and DST were the selected non-sulfurous agrochemical in a mixture of sulfurous ATC, SMB, TGA and SDDC were sensed. The absorption spectrum recorded under the same condition and represents an agglomeration of AuNS@CDPA only in presence of sulfur-based agrochemicals and also represents visible colour change. The agrochemicals having no sulfur element shows no sign of agglomeration and the observation was supported by UV-visible spectrum as represented in **Figure 4.7 (B-D)**.

4.3.3. Effect of pH and NaCl concentration

The pH of the analyte solution and its concentration can influence the sensing properties of the sensor and hence the behaviour of AuNS@CDPA under these conditions was evaluated by SPR absorption spectra. These studies were performed only on the Au derived sensor as the Ag sensor was not sensitive enough to detect the presence of either cysteine or SDDC.

Thus aggregation of AuNS@CDPA upon exposure to various buffer solutions in the range of pH 2 to 12 was analyzed in the presence as well as the absence of both the analytes (cysteine and SDDC) (**Figure 4.9 & Figure 4.10**). A self-aggregation of the sensor occurs at an acidic pH

value that is represented by SPR spectral changes and slight visual aggregation in the absence of analyte molecule cysteine[43]. However, in presence of cysteine, there were drastic changes in visual aggregation at pH 6. Further, a maximum SPR absorption ratio at A_{670}/A_{524} was also observed under pH 6 condition for cysteine. In the case of SDDC, the aggregation and maximum SPR absorption ratio occurred at pH 10. Hence pH 6 is the optimum pH for colourimetric assessment of cysteine and pH 10 for SDDC.

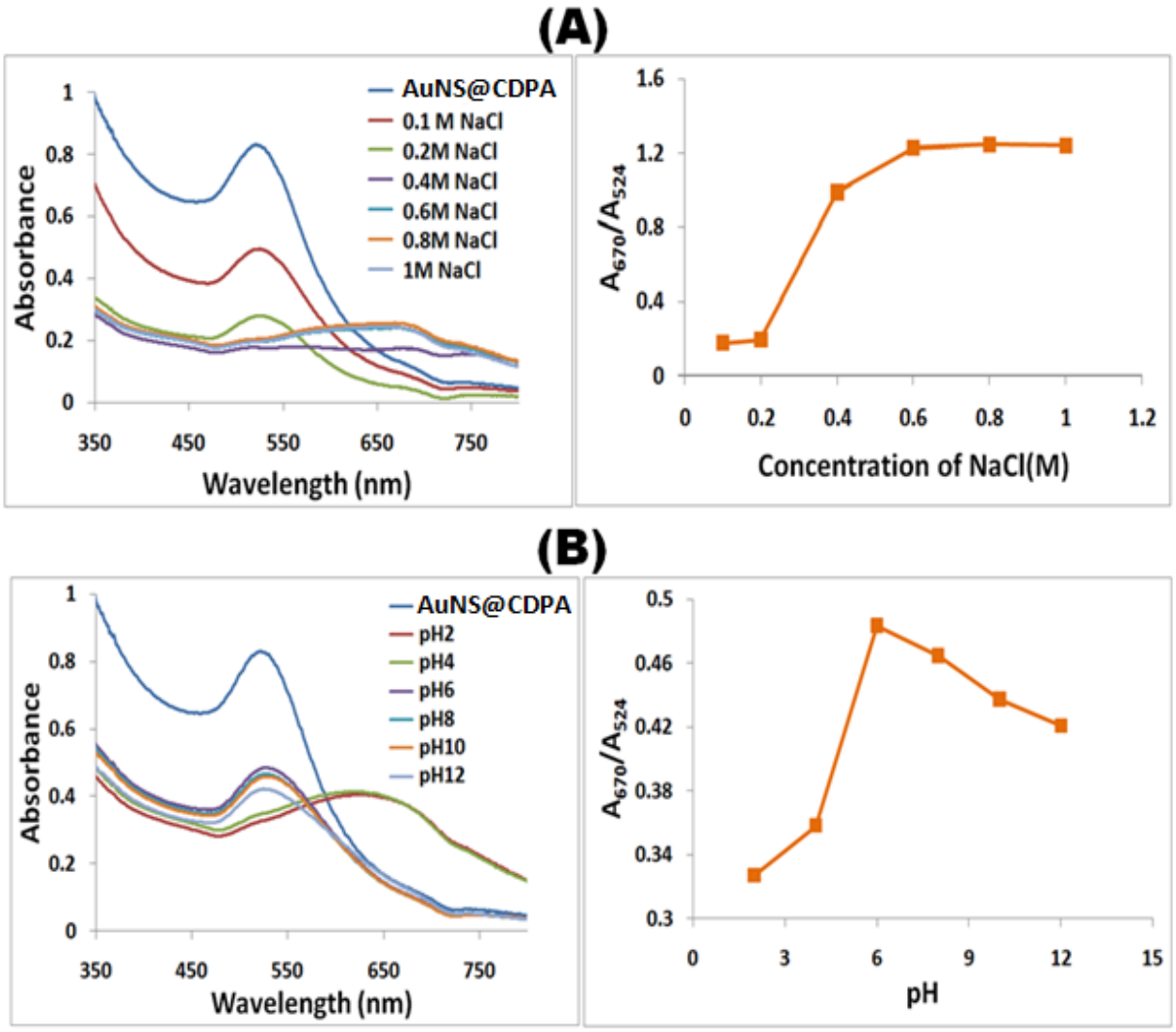

Figure 4.9: UV-visible spectra demonstrating effect of (A) NaCl concentration and (B) pH values in presence/absence of Cysteine. The graph of absorption ratio (A_{670}/A_{524}) versus NaCl concentration/pH shows the optimum sensing conditions

Similarly, the ionic strength effect on the sensing phenomenon was also studied. It was observed that, with increasing ionic strength, the shielding effect of NaCl triggers the aggregation of AuNS@CDPA in absence of analyte [44]. This phenomenon is termed the salting-out effect. The same phenomenon is observed even in the presence of the analyte. For the study in presence of cysteine, 1.0 mL of AuNS@CDPA was treated with various concentrations (0.1 to 1 M) of NaCl. As the concentration of NaCl increases, SPR peak intensity decreases whereas ratio A_{670}/A_{524} remains constant at 0.2 M NaCl for AuNS@CDPA.This occurs because the distance between adjacent gold nanoparticles decreases upon addition of NaCl resulting from a reduced electrostatic repulsion.

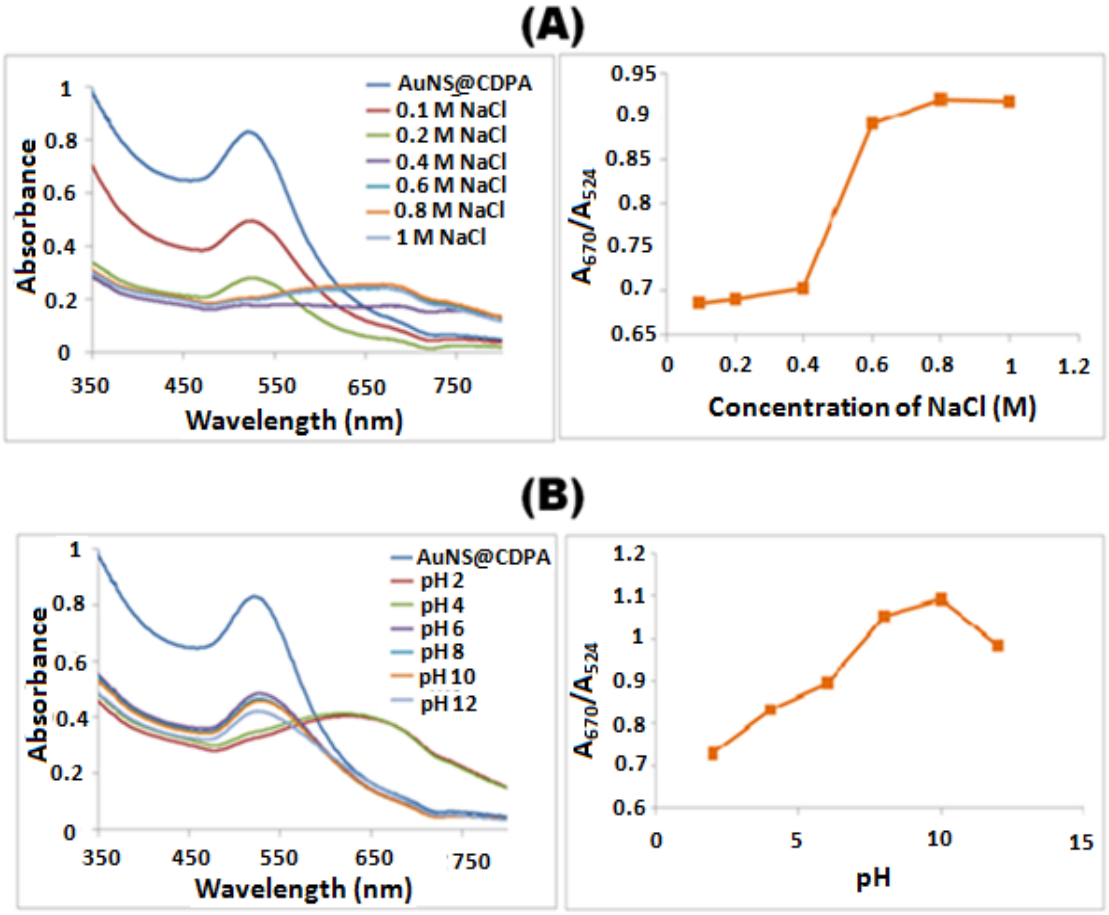

Figure 4.10: UV-visible spectra demonstrating effect of (A) NaCl concentration and (B) pH values in presence/absence of SDDC. The graph of absorption ratio (A_{670}/A_{524}) versus NaCl concentration/pH shows the optimum sensing conditions

4.3.4. Natural and real sample analysis

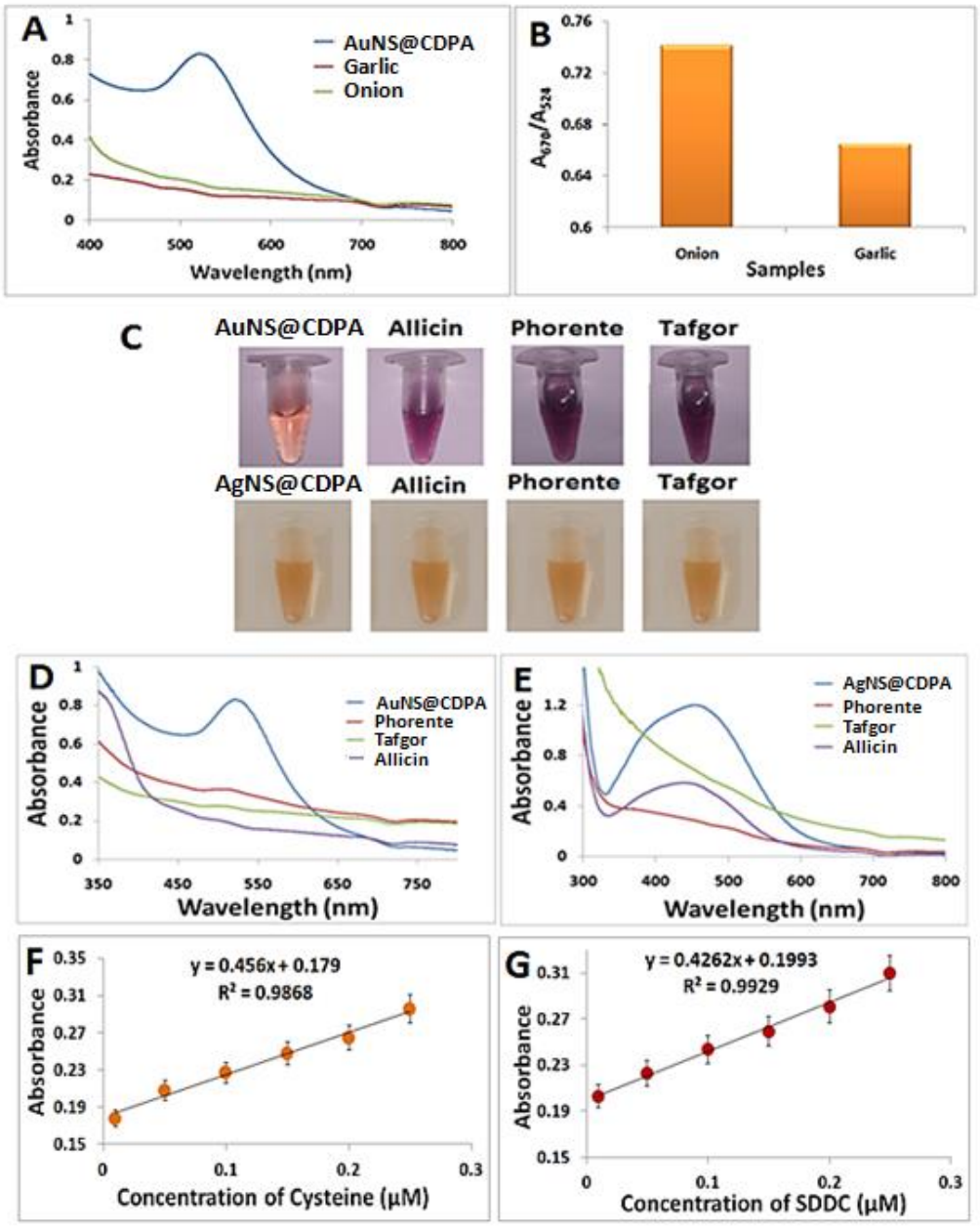

Figure 4.11: (A) UV-vis spectra and (B) Absorption ratio (A_{670}/A_{524}) of AuNS@CDPA in presence of allicin containing onion and garlic extract. (C)Photographs of AuNS@CDPA and AgNS@CDPA in presence of sulfur based pesticide samples and their (D&E) Absorption spectra. Linear relationship of (F) Cysteine and (G) SDDC with absorbance at 670 nm for quantification and determination of LOD (Sensing samples were prepared by adding 700 µL of AuNS@CDPA solution with 300 µL of different concentration of Cysteine

and SDDC, the error bars represent standard deviation obtained from three independent measurements).

Considering the potential of the sensor in sensing S rich compounds its capability of detecting natural and real samples were also assessed. Onion and garlic are known to contain sulfur-based compound "allicin" (thiosulfinate compound). Thus allicin was selected as a model natural component for detection. The onion and garlic extracts demonstrated a visual colour change from red to blue upon the addition of AuNS@CDPA and supported by UV-visible spectra as shown in **Figure 4.11 (A&B)**.

As the sensor was able to detect sulfur compounds in a complex extract matrix, the scope was further extended to the detection of hardcore sulfur pesticides utilized daily. For this study, Phorente and Tafgor were selected pesticides. They were spiked in known quantities in water samples and the sensitivity of AuNS@CDPA in their detection was investigated. A similar colour change from wine red to blue was observed in the case of both these pesticides agrochemicals as shown in **Figure 4.11 (C, D&E)**.

4.3.5. Selectivity and Sensitivity of AuNS@CDPA and AgNS@CDPA as a visible colourimetric detection system in a mixture of analytes

To detect the selectivity and sensitivity of the sensor towards S derived analytes the sensing experiments were carried out using several sulfur and non-sulfur analytes.

Firstly, the selectivity towards cysteine in a mixture of various amino acids was tested on AuNS@CDPA. The mixture of amino acids without cysteine did not show any change in either colour or absorption ratio. However, upon the addition of cysteine to the mixture, an agglomeration of the nanoparticles resulted in causing visual changes to the Au sensor solution. This is owing to the affinity of gold nanoparticles towards the S containing –SH group. On the other hand, the addition of a cysteine-containing amino acid mixture did not influence the spectral properties of AgNS@CDPA.

Similar studies were carried out by using various sulfated and non-sulfated agrochemical compounds. Various model agro compounds used for sensing were Potassium dihydrogen orthophosphate (PDO), Sodium dihydrogen orthophosphate (SDO), di-sodium tetraborate (DST), Sodium metabisulfite (SMB), di-ammonium hydrogen orthophosphate (DAHO), Sodium hypochloride (SHC), Diphenylamine (DPA)¸ Ammonium thiocyanate (ATC)¸ Thioglycolic acid

(TGA), Sodium diethyldithiocarbamate (SDDC). Out of the above-mentioned 10analytes, the colour change was observed only in the presence of sulfur containing4 such compounds namely ATC, SMB, SDDC and TGA. It is noteworthy that out of the 4 sulfated compounds, the sensor is most sensitive towards SDDC. For AuNS@CDPA to undergo a colour change by bathochromic shift, ATC, SMB and TGA were required in relatively higher concentrations of ~10 µM but SDDC was capable of inducing a colour change at 1000 times lower concentration of 0.01 µM. This may be attributed to the disulfide groups that can induce rapid agglomeration of gold nanoparticles. The addition of these again did not alter the spectral properties of AgNS@CDPA. Thus, the results clearly indicated that AuNS@CDPA has high selectivity towards sulfur-based compounds as compared to AgNS@CDPA.

The calibration plot of absorbance ratio vs. different concentrations for Cys and SDDC in the test range of 0.01-0.25 µM exhibited a fairly linear relationship with the lower limit of detection (LOD) of 0.05 and 0.07 µM for SDDC and Cys. The superiority of this method lies in facile readout and rapid visible colourimetric observations.

4.3.6. Analytical Performance

The detailed semi-quantitative and quantitative studies suggest that the presence of S containing model compounds like cysteine (amino acid) or SDDC (agrochemical) is capable of inducing aggregation of AuNS@CDPA. This is quantitatively proved from experiments that demonstrated an increasing absorption ratio i.e. A_{670}/A_{524} for cysteine and SDDC. Upon increasing the concentration of the added analytes (i.e. 0.01 -0.25 µM of cysteine and SDDC) led to a gradual colour change from red to blue. The spectra indicated a gradual increase in the intensity of blue colour with increasing concentration as reflected in the absorption spectral changes of AuNS@CDPA. The calculated correlation coefficient values of R^2= 0.995 for cysteine and R^2= 0.959 SDDC is proof of a good linear co-relation between absorption ratio in this concentration range as shown in **Figure 4.11 (F&G)**. The synthesized AuNS@CDPA is thus a biocompatible, non-toxic and cost-effective nano-sensor that can be employed for facile on-site detection purposes.

Such nanosensor possesses a comparatively better detection limit as compared to many paper-derived analytical devices. This is because despite being easy to employ, inexpensive and portable paper-based analytical sensors had bad limits of detection[19]. Thus AuNS@CDPA can be employed for the detection of S derived pollutants and agrochemicals under conditions of limited

resources owing to its rapid visual detectability and without the need for sample pre-treatment or pre-concentration.

Table 4.3: A comparison table of various Au/Ag derived nanosensors employed for colourimetric detection of cysteine/pesticides

Sr.No.	Nanosensor	Analyte	LOD	Reference
1.	Diphenylcarbazide capped Ag nanoparticles	Cysteine Homocysteine	0.16 µM 0.25 µM	[45]
2.	L-Aspartic acid capped Au nanoparticles	Cysteine	100 nM	[46]
3	Ractopamine hydrochloride stabilized Au nanoparticles	Cysteine	0.35 µM	[42]
4	Carboxymethyl cellulose-functionalized Au nanoparticles	Cysteine	10 µM	[47]
5.	Rhodamine B-functionalized Au nanoparticles	Pesticides Carbaryl Diazinon Malathion Phorate	 0.1 ppb 0.1 ppb 0.3 ppb 1.0 ppb	[8]
6.	Sodium dodecyl sulfate capped Ag nanoparticles	Dithiocarbamate pesticides Ziram Zineb Maneb	 149.3 ng/ml 4.0 ng/ml 9.1 ng/ml	[48]
7.	Citrate stabilized Au nanoparticles	Pesticide: Ametryn	0.15 ppb	[49]
8.	Silk fibroin gold nanocomposite	Pesticide: Chlorpyrifos	10 ppb	[31]
9	Cyclodextrin phthalate ester functionalized Au nanoparticles	Cysteine Agrochemical: SDDC	0.07 µM 0.05 µM	**This Work**

Table 4.3 demonstrates a comparison of the analytical performances of this nanosensor with some of the previously reported ones for the detection of either cysteine or agrochemicals. The assessment with previous work shows that the nanosensor employed in this work has LOD comparable with the other sensors. A much lower LOD value was noted for AuNS@CDPA as compared to some of the systems (Table entries 1-4). It is interesting to note that, although AuNS@CDPA has a greater LOD value than the systems mentioned in table entries 5 and 6 the merit of this approach lies in the use of a biocompatible non-toxic cyclodextrin polymer for the nanosensor design.

4.3.7. Mechanism

A strong affinity of gold for S plays a crucial role in the probable mechanism of action that is followed for the detection of the sulfurous analytes using AuNS@CDPA. In addition, the amphiphilic nature of cyclodextrin phthalate ester polymer that coats the AuNPs also has its role in the interaction of analytes with the sensor. **Figure 4.12 (A)** demonstrates the probable mechanism for cysteine sensing. Upon addition of AuNS@CDPA to a solution containing cysteine molecules, owing to it is hydrophilic nature the molecules tend to get entrapped in the hydrophilic part of the polymer network. The cysteine entrapment introduces the SH groups in the environment of AuNPs. Since gold has a strong affinity for SH groups, the phenomenon of ligand exchange is initiated and the AuNPs that was previously stabilized only carbonyl oxygen from polymer now interacts with SH groups of cysteine [50]. This increases the electrostatic forces of interaction between the polymer capped AuNPs and cysteine molecules as a consequence. This resulted in a decreased inter-particle distance between adjacent AuNPs and agglomeration occurs [51]. The agglomeration resulted in the changes in SPR absorbance and a bathochromic shift giving a visual readout in the form of colour change notifying the presence of cysteine.

Figure 4.12 (B) demonstrates the probable mechanism of SDDC interaction with the sensor. In the case of SDDC, the two methyl groups can get accommodated inside the cavity of cyclodextrin molecules owing to their hydrophobicity [52]. After being introduced in the sensor environment the S atoms in the structure of SDDC then interacts with Au molecules and induces aggregation via the same principle as described in the case of cysteine.

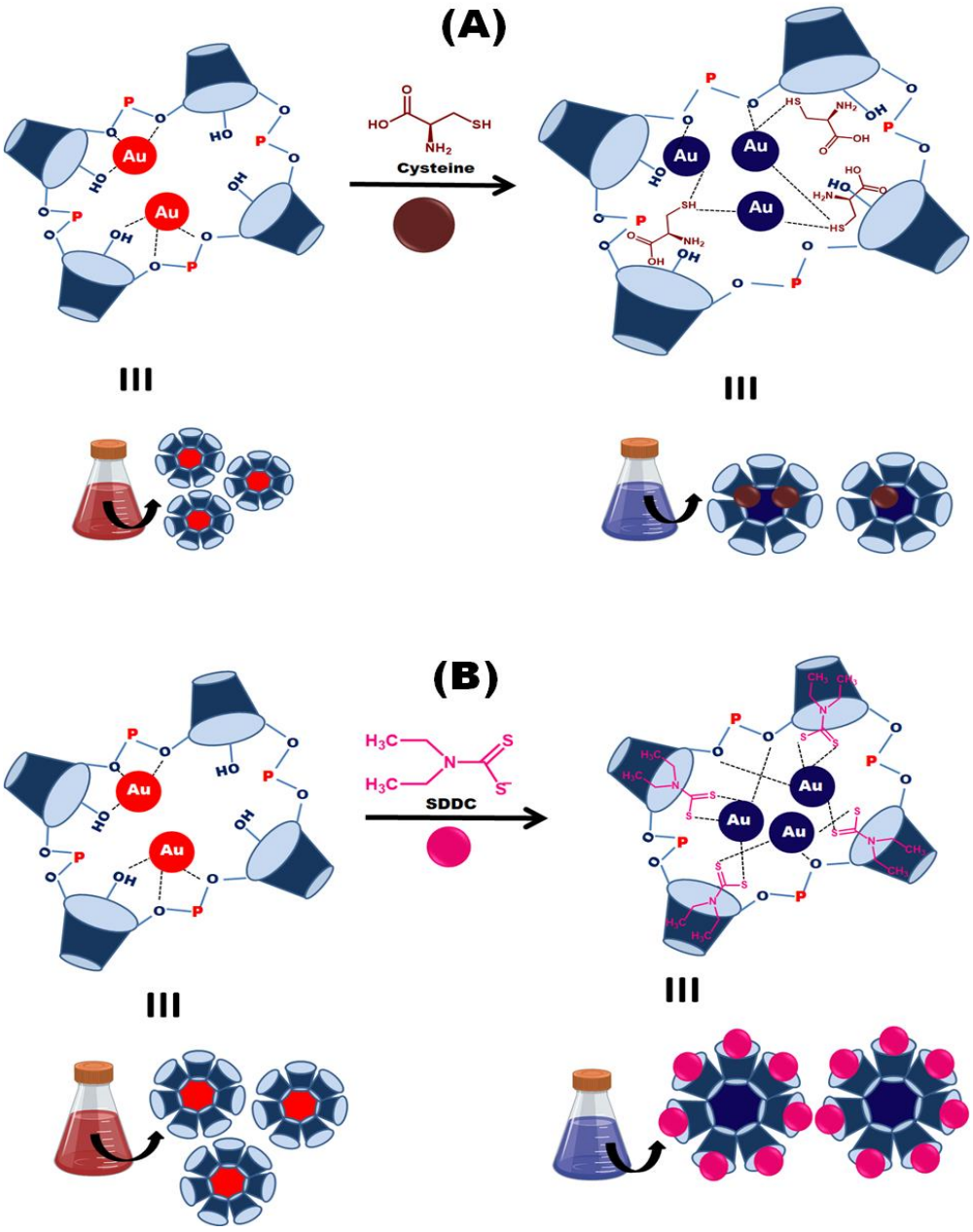

Figure 12: Schematic showing a probable mechanism for detection of (A) Cysteine and (B) SDDC using AuNS@CDPA

It is interesting to note that since SDDC can have interactions with the cavity whereas cysteine is entrapped in the hydrophilic environment, more SDDC molecules can have interaction with the sensor as compared to cysteine. This explains the improved sensitivity and low LOD value of AuNS@CDPA towards SDDC sensing in comparison with cysteine sensing.

The sensing mechanism is supported with various evidences from analytical characterizations like FTIR, HR-TEM and elemental mapping. The FTIR spectra demonstrated a new low-intensity peak at 2527 cm^{-1} in addition to the signature peaks of AuNS@CDPA that is representative of the presence of SH linkage of cysteine and its interaction with the AuNPs thereof (as shown in **Figure 4.13**) [53].

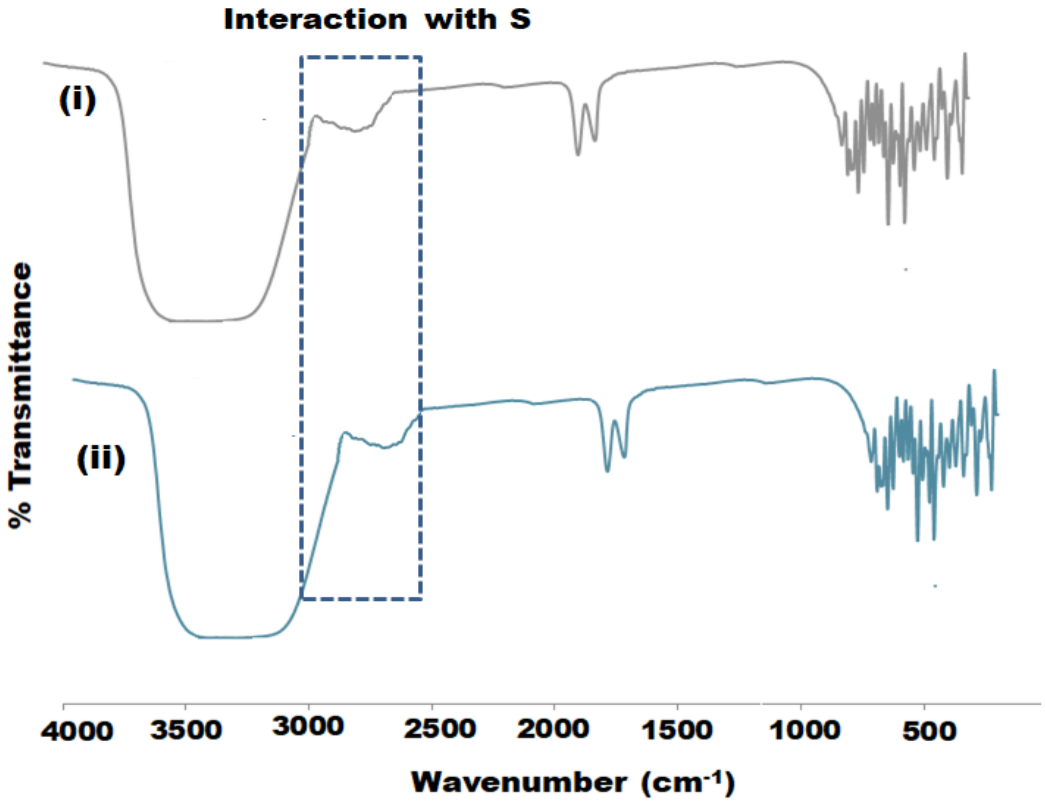

Figure 4.13: FTIR overlay spectra for AuNS@CDPA in presence of (i) Cysteine and (ii) SDDC

Similarly, in the case of SDDC the peak at 2521 cm^{-1} appears that is representative of S atoms interacting with AuNPs. The HRTEM images show an agglomeration and presence of large-sized aggregates in AuNS@CDPA upon addition of analyte molecules to the sensor solution. Upon addition of cysteine the size changes to 21 nm whereas in the case of SDDC, the size increases to 25 nm as shown in **Figure 4.14 (A&B)**. A large-sized aggregate in the case of SDDC as compared to cysteine again proves more interaction of SDDC with the sensor causing an enhanced agglomeration. On the other hand no change in the size of AgNS@CDPA proving no interaction of this sensor with the analytes (**Figure 4.14 (C&D)**).

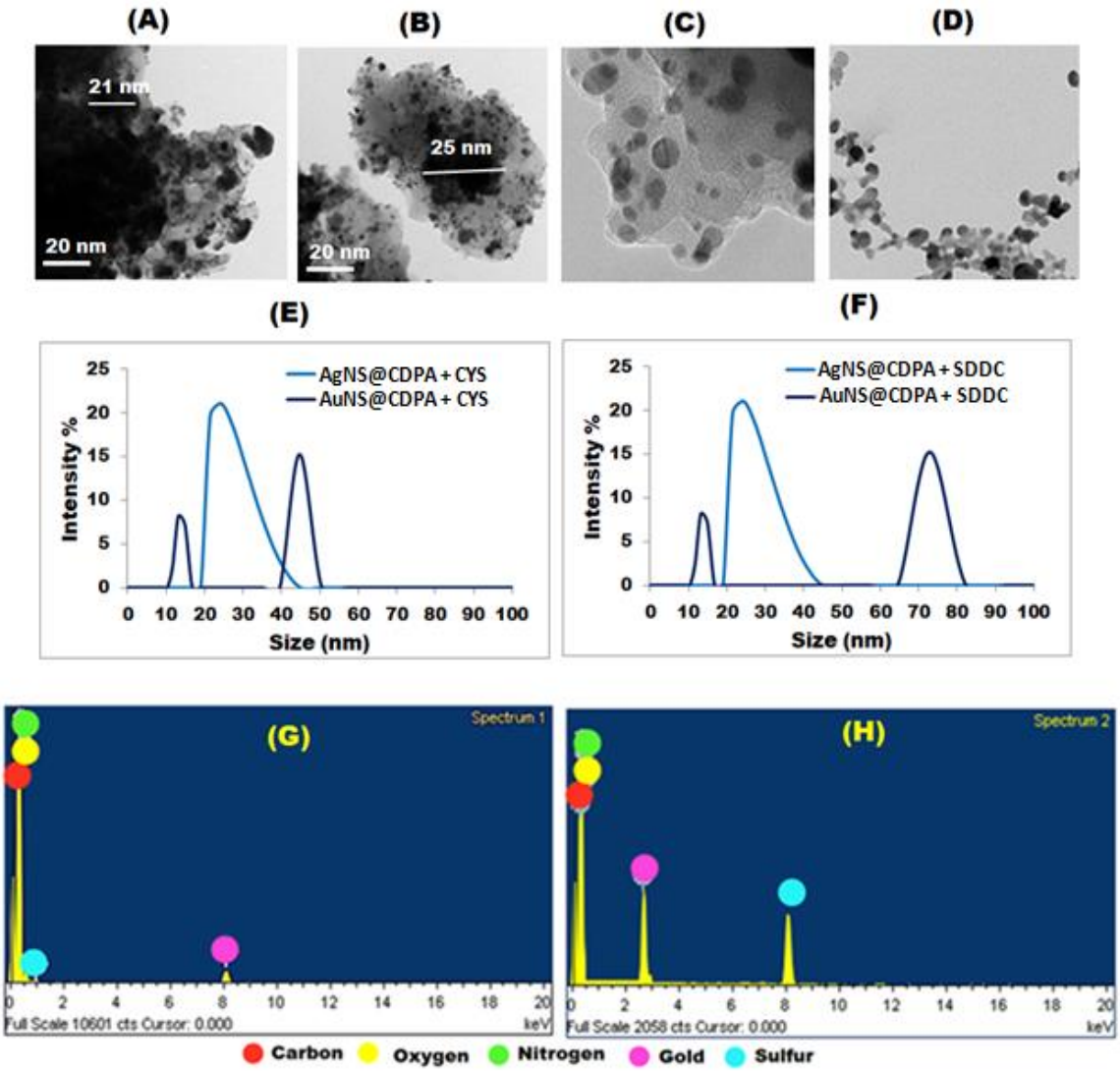

Figure 4.14: Various analytical characterization of sensor in presence of analytes; HRTEM image of (A) Cysteine added AuNS@CDPA (B) SDDC added AuNS@CDPA (C) Cysteine containing AgNS@CDPA and (D) SDDC containing AgNS@CDPA; (E) & (F) DLS spectra of Cysteine and SDDC containing sensor solutions; elemental mapping of (G) Cysteine and (H) SDDC added AuNS@CDPA

The results are corroborated by observations of DLS measurements. In addition to the presence of peaks at 13.2 nm for standard AuNS@CDPA, new peaks of large-sized aggregates are observed at 44.7 nm for cysteine and 72.8 nm in case of SDDC suggesting agglomeration in **Figure 4.14 (E&F)**. The hydrodynamic size of AgNS@CDPA however is not affected.

Elemental mapping shows the presence of S and N in the analyte added samples which are attributed to the presence of cysteine/SDDC (**Figure 4.14 (G&H)**).

Thus these characterizations support the probable mechanism proposed for sensing of S containing compounds using AuNS@CDPA.

4.4. Conclusion

To summarize, this work reports the synthesis of a biocompatible and nontoxic cyclodextrin derived polymer by its phthalylation. This polymer acts as both stabilizing and reducing agent for the synthesis of AuNPs and AgNPs, the resulting nanosystems are used as sensors for rapid detection of sulfated compounds. The polymer and sensors were thoroughly characterized by various analytical techniques. The microscopic imaging via FE-SEM and HRTEM suggest spherical morphology and formation of <15 nm-sized sensors. Elemental mapping revealed the presence of 12% elemental Au. Cysteine and SDDC have been used as model analytes to detect the efficiency of the nanosystems in sensing sulfur-based compounds. The colourimetric assessment is established on red shift (from 524 nm to 670 nm) within 5 seconds for sulfur-based compounds in the AuNS@CDPA system. The AgNS@CDPA however did not show any alteration in its spectral properties upon the addition of analytes. The effect of ionic strength and pH of solution on spectral characteristics of sensing has also been discussed. The quantitative studies suggested straight line linearity in the range of 0.01-0.25 µM for SDDC and Cysteine with LOD values of 0.05 and 0.07 µM respectively for these compounds. The sensitivity of AuNS@CDPA towards analyzing S compounds has been proved via analysis of various mixtures. The probable mechanism for sensing involving the role of CD's amphiphilicity in analyte entrapment and NP agglomeration has been shown with appropriate analytical evidence. The scope of the study was further extended to detecting real samples like analyzing allicin in complex extracts and real pesticide samples like phorente and tafgor. Thus AuNS@CDPA has been found to be a sensitive, rapid and effective colourimetric sensor giving visual readout instantaneously in presence of S compounds without the need for any sample preparation or pre-concentration. Thus AuNS@CDPA can be potential cost-effective nanoprobes that can be employed for sensing sulfated analytes.

References

(1) Muqeet, M.; Mahar, R. B.; Gadhi, T. A.; Ben Halima, N. Insight into Cellulose-Based-Nanomaterials - A Pursuit of Environmental Remedies. *Int. J. Biol. Macromol.* **2020**, *163*, 1480–1486. https://doi.org/10.1016/j.ijbiomac.2020.08.050.

(2) Jacob, J. M.; Karthik, C.; Saratale, R. G.; Kumar, S. S.; Prabakar, D.; Kadirvelu, K.; Pugazhendhi, A. Biological Approaches to Tackle Heavy Metal Pollution: A Survey of Literature. *J. Environ. Manage.* **2018**, *217*, 56–70. https://doi.org/10.1016/j.jenvman.2018.03.077.

(3) Yan, X.; Li, H.; Su, X. Review of Optical Sensors for Pesticides. *Trends Anal. Chem.* **2018**, *103*, 1–20. https://doi.org/10.1016/j.trac.2018.03.004.

(4) Saha, K.; Agasti, S. S.; Kim, C.; Li, X.; Rotello, V. M. Gold Nanoparticles in Chemical and Biological Sensing. *Chem. R* **2012**, *112* (5), 2739–2779.

(5) Kang, J.; Zhang, Y.; Li, X.; Miao, L.; Wu, A. A Rapid Colorimetric Sensor of Clenbuterol Based on Cysteamine-Modified Gold Nanoparticles. *ACS Appl. Mater. Interfaces* **2016**, *8* (1), 1–5. https://doi.org/10.1021/acsami.5b09079.

(6) Annu; Raja, A. N. Recent Development in Chitosan-Based Electrochemical Sensors and Its Sensing Application. *Int. J. Biol. Macromol.* **2020**, *164*, 4231–4244. https://doi.org/10.1016/j.ijbiomac.2020.09.012.

(7) Amjadi, M.; Hallaj, T.; Nasirloo, E. In Situ Formation of Ag/Au Nanorods as a Platform to Design a Non-Aggregation Colorimetric Assay for Uric Acid Detection in Biological Fluids. *Microchem. J.* **2020**, *154*, 104642. https://doi.org/https://doi.org/10.1016/j.microc.2020.104642.

(8) Liu, D.; Chen, W.; Wei, J.; Li, X.; Wang, Z.; Jiang, X. A Highly Sensitive, Dual-Readout Assay Based on Gold Nanoparticles for Organophosphorus and Carbamate Pesticides. *Anal. Chem.* **2012**, *84* (9), 4185–4191. https://doi.org/10.1021/ac300545p.

(9) Liu, Y.; Lv, B.; Liu, A.; Liang, G.; Yin, L.; Pu, Y.; Wei, W.; Gou, S.; Liu, S. Multicolor Sensor for Organophosphorus Pesticides Determination Based on the Bi-Enzyme

Catalytic Etching of Gold Nanorods. *Sensors Actuators, B Chem.* **2018**, *265*, 675–681. https://doi.org/10.1016/j.snb.2018.03.023.

(10) Nivethaa, E. A. K.; Dhanavel, S.; Narayanan, V.; Stephen, A. Chitosan Stabilized Ag-Au Nanoalloy for Colorimetric Sensing and 5-Fluorouracil Delivery. *Int. J. Biol. Macromol.* **2017**, *95*, 862–872. https://doi.org/10.1016/j.ijbiomac.2016.10.066.

(11) Saratale, R. G.; Saratale, G. D.; Ghodake, G.; Cho, S. K.; Kadam, A.; Kumar, G.; Jeon, B. H.; Pant, D.; Bhatnagar, A.; Shin, H. S. Wheat Straw Extracted Lignin in Silver Nanoparticles Synthesis: Expanding Its Prophecy towards Antineoplastic Potency and Hydrogen Peroxide Sensing Ability. *Int. J. Biol. Macromol.* **2019**, *128*, 391–400. https://doi.org/10.1016/j.ijbiomac.2019.01.120.

(12) Chen, H.; Zhang, L.; Hu, Y.; Zhou, C.; Lan, W.; Fu, H.; She, Y. Nanomaterials as Optical Sensors for Application in Rapid Detection of Food Contaminants, Quality and Authenticity. *Sensors Actuators B. Chem.* **2020**, *329*, 129–135. https://doi.org/10.1016/j.snb.2020.129135.

(13) Poosinuntakul, N.; Parnklang, T.; Sitiwed, T.; Chaiyo, S.; Kladsomboon, S.; Chailapakul, O.; Apilux, A. Colorimetric Assay for Determination of Cu (II) Ions Using l-Cysteine Functionalized Silver Nanoplates. *Microchem. J.* **2020**, *158*, 105101. https://doi.org/https://doi.org/10.1016/j.microc.2020.105101.

(14) Bankura, K.; Rana, D.; Mollick, M. M. R.; Pattanayak, S.; Bhowmick, B.; Saha, N. R.; Roy, I.; Midya, T.; Barman, G.; Chattopadhyay, D. Dextrin-Mediated Synthesis of Ag NPs for Colorimetric Assays of Cu2+ Ion and Au NPs for Catalytic Activity. *Int. J. Biol. Macromol.* **2015**, *80*, 309–316. https://doi.org/10.1016/j.ijbiomac.2015.06.058.

(15) Ravan, H.; Amandadi, M.; Hassanshahian, M.; Pourseyedi, S. Dual Catalytic DNA Circuit-Induced Gold Nanoparticle Aggregation: An Enzyme-Free and Colorimetric Strategy for Amplified Detection of Nucleic Acids. *Int. J. Biol. Macromol.* **2020**, *154*, 896–903. https://doi.org/10.1016/j.ijbiomac.2020.03.059.

(16) Zhang, J.; Mou, L.; Jiang, X. Surface Chemistry of Gold Nanoparticles for Health-Related Applications. *Chem. Sci.* **2020**, *11* (4), 923–936. https://doi.org/10.1039/c9sc06497d.

(17) Plácido, J.; Bustamante-lópez, S.; Meissner, K. E.; Kelly, D. E.; Kelly, S. L. Microalgae Biochar-Derived Carbon Dots and Their Application in Heavy Metal Sensing in Aqueous Systems. *Sci. Total Environ.* **2019**, *656*, 531–539. https://doi.org/10.1016/j.scitotenv.2018.11.393.

(18) Liu, L.; Li, Z.; Chen, C.; Shun, W. Visible Colorimetric Sensing of Cysteine Based on Au Nanoparticle Modified ZIF - 67. *Chem. Pap.* **2019**, *74*, 1839–1847. https://doi.org/10.1007/s11696-019-01032-0.

(19) Oliveira, E.; Núñez, C.; Santos, H. M.; Fernández-Lodeiro, J.; Fernández-Lodeiro, A.; Capelo, J. L.; Lodeiro, C. Revisiting the Use of Gold and Silver Functionalised Nanoparticles as Colorimetric and Fluorometric Chemosensors for Metal Ions. *Sensors Actuators, B Chem.* **2015**, *212*, 297–328. https://doi.org/10.1016/j.snb.2015.02.026.

(20) Chen, X.; Ji, J.; Wang, D.; Gou, S.; Xue, Z.; Zhao, L.; Feng, S. Highly Sensitive and Selective Colorimetric Sensing of Histidine by NAC Functionalized AuNPs in Aqueous Medium with Real Sample Application. *Microchem. J.* **2021**, *160*, 105661. https://doi.org/https://doi.org/10.1016/j.microc.2020.105661.

(21) Zhang, S.; Geng, Y.; Ye, N.; Xiang, Y. A Simple and Sensitive Colorimetric Sensor for Determination of Gentamicin in Milk Based on Lysine Functionalized Gold Nanoparticles. *Microchem. J.* **2020**, *158*, 105190. https://doi.org/https://doi.org/10.1016/j.microc.2020.105190.

(22) Thirumalraj, B.; Dhenadhayalan, N.; Chen, S. M.; Liu, Y. J.; Chen, T. W.; Liang, P. H.; Lin, K. C. Highly Sensitive Fluorogenic Sensing of L-Cysteine in Live Cells Using Gelatin-Stabilized Gold Nanoparticles Decorated Graphene Nanosheets. *Sensors Actuators, B Chem.* **2018**, *259*, 339–346. https://doi.org/10.1016/j.snb.2017.12.028.

(23) Sidhu, J. S.; Singh, A.; Garg, N.; Kaur, N.; Singh, N. Gold Conjugated Carbon Dots Nano Assembly: FRET Paired Fluorescence Probe for Cysteine Recognition. *Sensors Actuators, B Chem.* **2019**, *282*, 515–522. https://doi.org/10.1016/j.snb.2018.11.105.

(24) Devi, P.; Rajput, P.; Thakur, A.; Kim, K. Recent Advances in Carbon Quantum Dot-Based Sensing of Heavy Metals in Water. *Trends Anal. Chem.* **2019**, *114*, 171–195.

https://doi.org/10.1016/j.trac.2019.03.003.

(25) Yuan, Z.; Du, Y.; Tseng, Y. T.; Peng, M.; Cai, N.; He, Y.; Chang, H. T.; Yeung, E. S. Fluorescent Gold Nanodots Based Sensor Array for Proteins Discrimination. *Anal. Chem.* **2015**, *87* (8), 4253–4259. https://doi.org/10.1021/ac5045302.

(26) Cai, Y.; Hua, Y.; Yin, M.; Liu, H.; Li, S.; Wang, F.; Wang, H. Fabrication of Test Strips with Gold-Silver Nanospheres and Metal–Organic Frameworks: A Fluorimetric Method for Sensing Trace Cysteine in Hela Cells. *Sensors Actuators, B Chem.* **2020**, *302*, 127198. https://doi.org/10.1016/j.snb.2019.127198.

(27) Li, J. J.; Qiao, D.; Zhao, J.; Weng, G. J.; Zhu, J.; Zhao, J. W. Fluorescence Turn-on Sensing of L-Cysteine Based on FRET between Au-Ag Nanoclusters and Au Nanorods. *Spectrochim. Acta - Part A Mol. Biomol. Spectrosc.* **2019**, *217*, 247–255. https://doi.org/10.1016/j.saa.2019.03.092.

(28) Li, W.; Wen, X.; Zhao, H.; Yan, W.; Trant, J. F.; Li, Y. Acid-Triggered Self-Assembled Egg White Protein-Coated Gold Nanoclusters for Selective Fluorescent Detection of Fe^{3+}, NO^{2-}, and Cysteine. *ACS Appl. Nano Mater.* **2020**, *3* (12), 11838–11849. https://doi.org/10.1021/acsanm.0c02358.

(29) Nandi, I.; Chall, S.; Chowdhury, S.; Mitra, T.; Roy, S. S.; Chattopadhyay, K. Protein Fibril-Templated Biomimetic Synthesis of Highly Fluorescent Gold Nanoclusters and Their Applications in Cysteine Sensing. *ACS Omega* **2018**, *3* (7), 7703–7714. https://doi.org/10.1021/acsomega.8b01033.

(30) Wu, S.; Li, D.; Wang, J.; Zhao, Y.; Dong, S.; Wang, X. Gold Nanoparticles Dissolution Based Colorimetric Method for Highly Detection of Organophosphate Pesticides. *Sensors Actuators B. Chem.* **2017**, *238*, 472–433. https://doi.org/10.1016/j.snb.2016.07.067.

(31) Mane, P. C.; Shinde, M. D.; Varma, S.; Chaudhari, B. P. Highly Sensitive Label-Free Bio-Interfacial Colorimetric Sensor Based on Silk Fibroin-Gold Nanocomposite for Facile Detection of Chlorpyrifos Pesticide. *Sci. Rep.* **2020**, *10*, 1–14. https://doi.org/10.1038/s41598-020-61130-y.

(32) Kang, J.; Zhang, Y.; Li, X.; Dong, C.; Liu, H.; Miao, L.; Low, P. J.; Gao, Z.; Hosmane, N. S.; Wu, A. Rapid and Sensitive Colorimetric Sensing of the Insecticide Pymetrozine Using Melamine-Modified Gold Nanoparticles. *Anal. Methods* **2018**, *10*, 417–421. https://doi.org/10.1039/C7AY02658G.

(33) Hu, Y.; Wang, J.; Wu, Y. A Simple and Rapid Chemosensor for Colorimetric Detection of Dimethoate Pesticide Based on the Peroxidase-Mimicking Catalytic Activity of Gold. *Anal. Methods* **2019**, *11*, 5337–5347. https://doi.org/10.1039/c9ay01506j.

(34) Yadav, M.; Das, M.; Savani, C.; Thakore, S.; Jadeja, R. Maleic Anhydride Cross-Linked β - Cyclodextrin-Conjugated Magnetic Nanoadsorbent : An Ecofriendly Approach for Simultaneous Adsorption of Hydrophilic and Hydrophobic Dyes. *ACS Omega* **2019**, *4*, 11993–12003. https://doi.org/10.1021/acsomega.9b00881.

(35) Das, M.; Nariya, P.; Joshi, A.; Vohra, A.; Devkar, R.; Seshadri, S.; Thakore, S. Carbon Nanotube Embedded Cyclodextrin Polymer Derived Injectable Nanocarrier: A Multiple Faceted Platform for Stimulation of Multi-Drug Resistance Reversal. *Carbohydr. Polym.* **2020**, *247*, 116751. https://doi.org/10.1016/j.carbpol.2020.116751.

(36) Das, M.; Solanki, A.; Joshi, A.; Devkar, R.; Seshadri, S. β -Cyclodextrin Based Dual-Responsive Multifunctional Nanotheranostics for Cancer Cell Targeting and Dual Drug Delivery. *Carbohydr. Polym.* **2019**, *206*, 694–705. https://doi.org/10.1016/j.carbpol.2018.11.049.

(37) Sanderson, P. N.; Simpson, W.; Cubberley, R.; Aleksic, M.; Gutsell, S.; Russell, P. J. Mechanistic Understanding of Molecular Initiating Events (MIEs) Using NMR Spectroscopy. *Toxicol. Res. (Camb).* **2015**, *5* (1), 34–44. https://doi.org/10.1039/c5tx00246j.

(38) Yorseng, K.; Siengchin, S.; Ashok, B. Nanocomposite Egg Shell Powder with in Situ Generated Silver Nanoparticles Using Inherent Collagen as Reducing Agent. *J. Bioresour. Bioprod.* **2020**, *5* (2), 101–107. https://doi.org/10.1016/j.jobab.2020.04.003.

(39) Ashok, B.; Hariram, N.; Siengchin, S.; Rajulu, A. V. Modification of Tamarind Fruit Shell Powder with in Situ Generated Copper Nanoparticles by Single Step Hydrothermal

Method. *J. Bioresour. Bioprod.* **2020**, *5* (3), 180–185. https://doi.org/10.1016/j.jobab.2020.07.003.

(40) Naceur Abouloula, C.; Rizwan, M.; Selvanathan, V.; Hassan, A.; Yahya, R.; Oueriagli, A. Oil Palm Waste Based Phthaloyl Cellulose: A Product of Photosynthesis as an Electrolyte of Photovoltaics. *Cellulose* **2019**, *26* (3), 1605–1617. https://doi.org/10.1007/s10570-018-2204-6.

(41) Nariya, P.; Das, M.; Shukla, F.; Thakore, S. Synthesis of Magnetic Silver Cyclodextrin Nanocomposite as Catalyst for Reduction of Nitro Aromatics and Organic Dyes. *J. Mol. Liq.* **2020**, *300*, 112279. https://doi.org/10.1016/j.molliq.2019.112279.

(42) Kateshiya, M. R.; George, G.; Rohit, J. V; Malek, N. I.; Kailasa, S. K. Ractopamine as a Novel Reagent for the Fabrication of Gold Nanoparticles: Colorimetric Sensing of Cysteine and Hg^{2+} Ion with Different Spectral Characteristics. *Microchem. J.* **2020**, 105212. https://doi.org/10.1016/j.microc.2020.105212.

(43) Wang, J.; Li, Y. F.; Huang, C. Z.; Wu, T. Rapid and Selective Detection of Cysteine Based on Its Induced Aggregates of Cetyltrimethylammonium Bromide Capped Gold Nanoparticles. *Anal. Chim. Acta* **2008**, *626* (1), 37–43. https://doi.org/10.1016/j.aca.2008.07.037.

(44) Bhamore, J.; Rawat, K. A.; Basu, H.; Singhal, R. K.; Kailasa, S. K. Influence of Molecular Assembly and NaCl Concentration on Gold Nanoparticles for Colorimetric Detection of Cysteine and Glutathione. *Sensors Actuators, B Chem.* **2015**, *212*, 526–535. https://doi.org/10.1016/j.snb.2015.01.133.

(45) Shariati, S.; Khayatian, G. The Colorimetric and Microfluidic Paper-Based Detection of Cysteine and Homocysteine Using 1,5-Diphenylcarbazide-Capped Silver Nanoparticles. *RSC Adv.* **2021**, *11* (6), 3295–3303. https://doi.org/10.1039/d0ra08615k.

(46) Qian, Q.; Deng, J.; Wang, D.; Yang, L.; Yu, P.; Mao, L. Aspartic Acid-Promoted Highly Selective and Sensitive Colorimetric Sensing of Cysteine in Rat Brain. *Anal. Chem.* **2012**, *84*, 9579–9584. https://doi.org/10.1021/ac3024608.

(47) Wei, X.; Qi, L.; Tan, J.; Liu, R.; Wang, F. A Colorimetric Sensor for Determination of Cysteine by Carboxymethyl Cellulose-Functionalized Gold Nanoparticles. *Anal. Chim. Acta* **2010**, *671* (1–2), 80–84. https://doi.org/10.1016/j.aca.2010.05.006.

(48) Ghoto, S. A.; Khuhawar, M. Y.; Jahangir, T. M. Silver Nanoparticles with Sodium Dodecyl Sulfate as Colorimetric Probe for Detection of Dithiocarbamate Pesticides in Environmental Samples. *Anal. Sci.* **2019**, *35* (6), 631–637. https://doi.org/10.2116/analsci.18P417.

(49) Qu, Y.; Qian, H.; Mi, Y.; He, J.; Gao, H.; Lu, R.; Zhang, S.; Zhou, W. Rapid Determination of the Pesticide Ametryn Based on a Colorimetric Aptasensor of Gold Nanoparticles. *Anal. Methods* **2020**, *12* (14), 1919–1925. https://doi.org/10.1039/d0ay00283f.

(50) Lodha, A.; Pandya, A.; Sutariya, P.; Menon, S. K. A Smart and Rapid Colorimetric Method for Detection of Codeine Sulphate, Using Unmodified Gold Nanoprobe. *RSC Adv.* **2014**, *4*, 50443–50448. https://doi.org/10.1039/c0xx00000x.

(51) Li, L.; Liao, L.; Ding, Y.; Zeng, H. Dithizone-Etched CdTe Nanoparticles-Based Fluorescence Sensor for the off-on Detection of Cadmium Ion in Aqueous Media. *RSC Adv.* **2017**, *7* (17), 10361–10368. https://doi.org/10.1039/C6RA24971J.

(52) Suliman, A. S.; Khoder, M.; Tolaymat, I.; Webster, M.; Alany, R. G.; Wang, W.; Elhissi, A.; Najlah, M. Cyclodextrin Diethyldithiocarbamate Copper Ii Inclusion Complexes: A Promising Chemotherapeutic Delivery System against Chemoresistant Triple Negative Breast Cancer Cell Lines. *Pharmaceutics* **2021**, *13* (1), 84. https://doi.org/10.3390/pharmaceutics13010084.

(53) Pandya, A.; Sutariya, P. G.; Lodha, A.; Menon, S. K. A Novel Calix[4]Arene Thiol Functionalized Silver Nanoprobe for Selective Recognition of Ferric Ion with Nanomolar Sensitivity via DLS Selectivity in Human Biological Fluid. *Nanoscale* **2013**, *5* (6), 2364–2371. https://doi.org/10.1039/c3nr33119a.

Paper Published from this Chapter:

Microchemical Journal 169 (2021) 106630

Contents lists available at ScienceDirect

Microchemical Journal

journal homepage: www.elsevier.com/locate/microc

Rapid selective optical detection of sulfur containing agrochemicals and amino acid by functionalized cyclodextrin polymer derived gold nanoprobes

Monika Yadav [a,1], Manita Das [b,1], Shivangi Bhatt [b], Pranav Shah [d], Rajendrasinh Jadeja [a,b,*], Sonal Thakore [b,c,*]

[a] Department of Environmental Studies, Faculty of Science, The Maharaja Sayajirao University of Baroda, Vadodara 390 002, India
[b] Department of Chemistry, Faculty of Science, The Maharaja Sayajirao University of Baroda, Vadodara 390 002, India
[c] Institute of Interdisciplinary Studies, The Maharaja Sayajirao University of Baroda, Vadodara 390 002, India
[d] Department of Pharmaceutics and Pharmaceutical Technology, Maliba Pharmacy College, UkaTarsadia University, Maliba Campus, Surat 394350, India

ARTICLE INFO

Keywords:
Visual sensing
Crosslinked cyclodextrin
LSPR band
Gold nanoparticles
Cysteine
Allicin

ABSTRACT

Rapid and accurate evaluation of sulfur-based pollutant contamination in an aqueous solution is one of the major tasks in environmental monitoring. A novel cyclodextrin phthalate ester polymer was used to synthesize gold and silver nanoparticles (NPs) with less than 15 nm size. The potential of the NPs solutions as chemosensor was assessed for the colourimetric detection of sulfur-based compounds. An agglomeration of only gold nanoparticles was induced selectively upon interaction with cysteine and sodium diethyldithiocarbamate (SDDC) leading to visual readout. The sensing, as well as quantification of cysteine (hydrophilic) and sodium diethyldithiocarbamate (SDDC) compounds (hydrophobic), occurred within seconds due to the dual binding ability of cyclodextrin. The limit of detection was determined using the linearity of absorbance plots. The proof of concept experiments demonstrates the rapid colourimetric determination in the range of 0.01–0.25 μM with a satisfactory limit of detection as 0.05 and 0.07 μM for SDDC and Cysteine respectively. The effect of pH and NaCl concentration on sensing was also investigated and optimized. 6 and 10 are the optimum pH values for the determination of cysteine and SDDC respectively. The optimum salt concentration was found to be 0.02 M for both the analytes. AuNPs nanosensor was much superior to AgNPs nanosensor as Au has an affinity for sulfur groups thus assisting a selective detection of cysteine and sulfur-containing pesticides in aqueous medium as well as allicin from onion and garlic extract.

1. Introduction

Chemical toxins, pesticides, heavy metals, organic-inorganic pollutants etc. are released in water via natural or anthropogenic processes [1]. They require persistent monitoring to secure a better supply of water in the public domain and also to administer their effect on the environment and ecosystem [2]. Recognition of chemical and biological agents present in the environment play a crucial role in forensic, biomedical and environmental sciences applications [3–7]. The techniques like atomic absorption spectroscopy, electrochemical sensors, inductively coupled plasma atomic emission spectrometry etc. exhibit low detection limits but are time-consuming, expensive, complex, sample destructive. Thus sophisticated instrument-based methods and not suitable for on-site detection [8]. On the other hand, chemosensors and molecular probes based on colourimetric and fluorometric methods are popular due to operational simplicity. They employ visual readout methods that rely on unique optical properties of noble metal nanomaterials such as surface plasmon resonance (SPR) [9–11]. Sensors generally possess two functional components i.e. a recognition element that binds specifically with analytes and a component i.e. transducer which signals the binding process. The efficiency of the sensor depends upon the above-mentioned components for significant sensing based on response time, the limit of detection, selectivity etc. Hence, the synthesis of the sensor having high efficacy relies on the generation of new

* Corresponding authors at: Department of Chemistry, Faculty of Science, The Maharaja Sayajirao University of Baroda, Vadodara 390 002, India.
E-mail addresses: chemistry2797@yahoo.com, drsonalit@gmail.com (R. Jadeja), rjadeja-chem@msubaroda.ac.in (S. Thakore).
[1] These authors contributed equally to this work.

https://doi.org/10.1016/j.microc.2021.106630
Received 14 May 2021; Received in revised form 6 July 2021; Accepted 7 July 2021
Available online 11 July 2021